

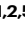







Timely lagging strand maturation relies on Ubp10 deubiquitylase-mediated PCNA dissociation from replicating chromatin

Received: 5 January 2024

Accepted: 11 September 2024

Published online: 18 September 2024

 Check for updatesJavier Zamarreño ^{1,2,5}, Sofía Muñoz ^{1,2,4,5}, Esmeralda Alonso-Rodríguez ^{1,2,5}, Macarena Alcalá ^{1,2}, Sergio Rodríguez ^{1,2}, Rodrigo Bermejo ³, María P. Sacristán ^{1,2} ✉ & Avelino Bueno ^{1,2} ✉

Synthesis and maturation of Okazaki Fragments is an incessant and highly efficient metabolic process completing the synthesis of the lagging strands at replication forks during S phase. Accurate Okazaki fragment maturation (OFM) is crucial to maintain genome integrity and, therefore, cell survival in all living organisms. In eukaryotes, OFM involves the consecutive action of DNA polymerase Pol δ , 5' Flap endonuclease Fen1 and DNA ligase I, and constitutes the best example of a sequential process coordinated by the sliding clamp PCNA. For OFM to occur efficiently, cooperation of these enzymes with PCNA must be highly regulated. Here, we present evidence of a role for the K164-PCNA-deubiquitylase Ubp10 in the maturation of Okazaki fragments in the budding yeast *Saccharomyces cerevisiae*. We show that Ubp10 associates with lagging-strand DNA synthesis machineries on replicating chromatin to ensure timely ligation of Okazaki fragments by promoting PCNA dissociation from chromatin requiring lysine 164 deubiquitylation.

The *POL30* gene of *Saccharomyces cerevisiae* encodes the sliding clamp PCNA (Proliferating Cell Nuclear Antigen), a conserved ring-shaped protein with essential roles in DNA metabolism as a crucial component of replication and repair machineries. PCNA forms a homotrimer that encircles DNA, where it interacts with a staggering number of proteins involved in every step required for DNA replication or repair. Thus, whereas it is devoid of enzymatic activity itself, PCNA exerts its function by recruiting and, in many instances, also activating numerous interactors^{1,2}.

DNA polymerases require free 3'-OH groups to initiate DNA synthesis, therefore, they can only synthesize DNA in a 5'-3' direction. As a result of this and the antiparallel nature of double stranded DNA, replication of one of the strands is discontinuous through the generation of Okazaki Fragments (OF). This strand is called the lagging strand (in contrast to the leading one). PCNA plays a crucial role in the

synthesis and maturation of these OFs. Thus, PCNA is loaded on dsDNA at primer-template junctions to recruit Pol δ and enhance its processivity. When the Pol δ -PCNA complex collides with the 5'-end of the preceding OF, it displaces a short flap that is cleaved off by the structure-specific flap endonuclease-1 Fen1, Rad27 in *S. cerevisiae*, upon binding to PCNA. This process generates a nick in the nascent DNA that is sealed by DNA ligase I, Cdc9 in *S. cerevisiae*, which is also recruited and catalytically activated through its interaction with PCNA³. All three subunits of DNA Pol δ , Fen1/Rad27, and DNA ligase I/Cdc9 harbor PIP (PCNA-interacting peptide)-boxes, through which they interact in a coordinated manner with the Inter-Domain Connecting Loop (IDCL) of PCNA, a major interaction site in the sliding clamp⁴⁻⁶. Although the mechanisms and factors involved in lagging strand maturation have been extensively studied key molecular details of OF maturation remain poorly understood.

¹Instituto de Biología Molecular y Celular del Cáncer (IBMCC), Universidad de Salamanca-CSIC, Campus Miguel de Unamuno, Salamanca, Spain. ²Departamento de Microbiología y Genética, Universidad de Salamanca, Campus Miguel de Unamuno, Salamanca, Spain. ³Centro de Investigaciones Biológicas "Margarita Salas", CSIC, Madrid, Spain. ⁴Present address: Instituto de Biología Funcional y Genómica (IBFG), CSIC-Universidad de Salamanca, Salamanca, Spain. ⁵These authors contributed equally: Javier Zamarreño, Sofía Muñoz, Esmeralda Alonso-Rodríguez. ✉ e-mail: msacristan@usal.es; abn@usal.es

To ensure the successful completion of DNA replication, particularly of the processive synthesis of the lagging strands, continuous recycling of chromatin-bound PCNA is required. The sliding clamp is loaded when required and actively unloaded when no longer needed in order to suppress illegitimate enzymatic reactions^{2,7,8}. RFC (Replication factor C) and RFC-like complexes (RLCs) mediate the loading and unloading of PCNA (reviewed in ref. 9). There is a general consensus regarding Rfc1-RFC complex role as the main loader of PCNA on replicating chromatin^{10,11}. One additional complex, Ctf18-RLC, also acts as a PCNA loader, although Ctf18 cannot substitute Rfc1. Moreover, Rfc1 and Ctf18 show a strand preference during replication, with a lagging strand bias for Rfc1 and a slight leading strand preference for Ctf18^{12–14}. Both Rfc1 and Ctf18 also exhibit some ability to unload PCNA in vitro. Human Rfc1-RFC, but not yeast Rfc1, is able to unload PCNA in vitro in an ATP-dependent manner^{15,16} and yeast Ctf18-RLC promotes an in vitro PCNA unloading mechanism, that also requires ATP hydrolysis, in the presence of ssDNA coated with RPA¹⁷. Despite these in vitro results, PCNA unloading activities for Rfc1- or Ctf18- complexes in vivo have not been reported.

Elg1-RLC complex (ATAD5-RLC in mammals) is considered as the major PCNA unloader when the role of PCNA in DNA replication is completed^{8,18–22}. However, given that *ELG1* is a non-essential gene for cell division^{23–25} and that PCNA accumulated in Elg1-depleted cells ends up being removed from chromatin before M phase^{18,20}, it is likely that additional PCNA unloaders are required during chromosome replication, at least in the absence of Elg1. Therefore, it remains unclear whether Elg1-RLC is the only in vivo PCNA unloader^{22,26}.

PCNA functions are regulated by different post-translational modifications such as SUMOylation, ubiquitylation, phosphorylation or acetylation, which confer PCNA the necessary plasticity to interact with its different binding partners^{1,27,28}. In the face of DNA lesions, PCNA is ubiquitylated to mediate damage-tolerance mechanisms that allow circumventing DNA lesions and prevent replication fork stalling^{29,30}. PCNA is mono-ubiquitylated at K164 by the evolutionary conserved RAD6/RAD18 (E2/E3) ubiquitin ligase complex to switch its affinity from replicative polymerases to damage-tolerant translesion synthesis (TLS) DNA polymerases, which, although mutagenic, are capable to bypass damaged bases^{27,31,32}. Furthermore, polyubiquitylation of the same residue by the Rad5/Mms2/Ubc13 PCNA-ubiquitin ligase complex leads to template switching (TS), the DNA damage tolerance (DDT) error-free pathway, to overcome the potentially lethal effects of replication fork stalling^{27,30}. We and others reported that the precise regulation of these processes not only depends on writer enzymes, PCNA^{K164}-Ubiquitin ligase complexes, but also on the erasers of these modifications. Thus, both TLS and TS pathways are limited by PCNA-deubiquitylation processes to minimize their deleterious cellular side effects. In mammals, deubiquitylating enzymes Usp1, Usp7, and Usp10 revert PCNA ubiquitylation caused in response to DNA damage^{28,33–35}. Knockdown of *USP1* induces aberrant PCNA mono-ubiquitylation, enhanced recruitment of error-prone TLS polymerases and increased mutagenesis levels in human cells^{33,35}. In the case of the budding yeast *S. cerevisiae*, the PCNA-DUBs Ubp10 and Ubp12^{36,37} limit the extent of DDT processes during the progression of exogenously unperturbed S phase by reverting K164-ubiquitylation of the sliding clamp at replication forks³⁷. Ubp10 ubiquitin-protease has also a role deubiquitylating histone H2B^{K123} working at genomics sites distinct of the SAGA-related histone H2B^{K123} DUB Ubp8 sites^{38–40}. Moreover, Ubp10 activity is also involved in the regulation of RNA polymerase I stability⁴¹. Remarkably, despite the key roles of this PCNA-DUB, abrogation of the *UBP10* gene is viable, even though *ubp10* mutated cells have both growth and cell cycle progression defects^{36,37,41,42}. Suppression of either growth or cell cycle defects can be accomplished by mutation of specific targets. Thus, multiple deletion of the TLS polymerases (*REV1*, *REV3* and *RAD30*) rescues the cell cycle delay in S phase progression caused by the abrogation of Ubp10³⁷, indicating that the

role of Ubp10 in supporting normal replication rates through PCNA-K164 deubiquitylation is dependent, at least in part, on the TLS pathway.

A number of active roles in the regulation of key cellular mechanisms has been described for ubiquitin-signaling writers, but not so many for erasers. Along this line of thought, it is assumed that pivotal regulatory steps rest on ubiquitin writers while partly redundant erasers were considered to act automatically or spontaneously after the post-translational modification is added to a given substrate. For these reasons ubiquitin proteases were in general considered to play a minor role, if any, in regulatory controls. In this context, it is assumed that PCNA ubiquitylation is counteracted by constitutive deubiquitylation mediated by PCNA-DUBs^{43,44}. However, recent work with yeast models concerning PCNA-DUBs role in DNA replication shows that something is amiss with this scenario both in fission and budding yeast^{37,43}. Regarding this matter, Ubp10 has a remarkable slow S phase phenotype that we were very interested to understand in full.

PCNA^{K164} ubiquitylation has also been linked to the OFM process. Thus, loss of PCNA ubiquitylation seems to cause inefficient gap-filling which interferes with efficient OF ligation in fission yeast and human cells^{44,45}. Moreover, PCNA^{K164} ubiquitylation suppresses replication stress resulting from Fen1/Rad27-defective flap processing during OFM⁴⁶, and the PCNA^{K164R} mutant shows inefficient OF processing in an in vitro DNA replication reconstitution assay using yeast proteins⁴⁷. Here, we present evidence of the role of Ubp10 in the regulation of OFM. Mass spectrometry analysis of the Ubp10 interactome showed that this PCNA-DUB interacts with all major components of the OF metabolism. Based on this observation and on the cell cycle delay in S phase, characteristic of cells deficient in Ubp10, we focused on deciphering the potential link between Ubp10 and OFM processes. Ablation of Ubp10 leads to accumulation of unligated OFs and a markedly increase of chromatin-bound PCNA during S phase. *POL30* mutants that conform unstable PCNA homotrimers on chromatin, particularly *pol30*^{R14E} and *pol30*^{D150E} alleles, counteract these *ubp10Δ*-associated replication defects, as well as cell cycle delay. In addition, abrogation of *ubp10* is strongly additive to *elg1* depletion, resulting in substantial increase of the PCNA bound to chromatin during replication. Slow S-phase and PCNA accretion on chromatin in *ubp10* cells is suppressed by non-ubiquitylatable K164 PCNA alleles. These data indicate that timely dissociation of PCNA during lagging strand synthesis requires action of the Ubp10 DUB to promote PCNA unloading. Collectively, this evidence reveals an important regulatory role for Ubp10 at the lagging strand synthesis.

Results

PCNA-DUB Ubp10 physically interacts with core components of the lagging-strand synthesis machinery

We first analyzed the interactome of the H2B- and PCNA-ubiquitin protease Ubp10 to reveal partners of this DUB during DNA replication by LC-MS-MS analysis. Mass spectrometry analysis of the proteome associated with Ubp10 in unperturbed S phase cells retrieved all major components of the lagging strand synthesis machinery (such as PCNA, Pol α /primase, RFC replication clamp loader, DNA polymerase δ) and Okazaki fragment metabolism (Fen1 flap endonuclease, Cdc9 ligase, RNase H2) (Table 1). A complementary proteomic analysis of DNA ligase Cdc9 also revealed Ubp10 as one of the DNA ligase interactors (to be published elsewhere). Relevant interactions were confirmed by direct co-immunoprecipitation (ChIP-CoIP) analyzes in epitope-tagged backgrounds, as shown for Pol3, catalytic subunit of Pol δ , (Supplementary Fig. 1A), and Cdc9 (Supplementary Fig. 1B). Ubp10-PCNA and Ubp10-Fen1 ChIP-CoIP interactions have been described previously^{36,37}. This evidence suggests the existence of a functional link between Pol δ , Fen1, Cdc9, Ubp10 and PCNA, and, therefore, supports the hypothesis that Ubp10 works on the lagging strand during OFM. Likely significant, our Ubp10-GFP-trap proteomic approach did not detect RLC cofactor Elg1. In contrast, all Rfc1-RFC

Table 1 | PCNA-DUB Ubp10 interacts with core components of lagging-strand synthesis machinery

Selected Identified interactors	Gene names	Score	Unique peptides
DNA primase small subunit	<i>PRI1</i>	12	5
DNA primase large subunit	<i>PRI2</i>	21	4
DNA polymerase α	<i>POL1</i>	26	6
DNA polymerase α subunit	<i>POL12</i>	32	9
DNA pol α -binding protein	<i>CTF4</i>	39	8
Replication factor C subunit 1	<i>RFC1</i>	38	10
Replication factor C subunit 2	<i>RFC2</i>	111	13
Replication factor C subunit 3	<i>RFC3</i>	118	12
Replication factor C subunit 4	<i>RFC4</i>	85	10
Replication factor C subunit 5	<i>RFC5</i>	70	13
PCNA	<i>POL30</i>	76	10
DNA polymerase δ	<i>POL3</i>	32	9
DNA polymerase δ subunit	<i>POL31</i>	23	5
FLAP endonuclease I	<i>FEN1/RAD27</i>	34	8
DNA ligase I	<i>CDC9</i>	22	7
Replication factor A protein 1	<i>RFA1</i>	98	12
Replication factor A protein 2	<i>RFA2</i>	38	5
Replication factor A protein 3	<i>RFA3</i>	61	3
Ribonuclease H2 subunit A	<i>RNH201</i>	22	6
Ribonuclease H2 subunit B	<i>RNH202</i>	54	9
DNA mismatch repair protein	<i>MSH2</i>	34	10
DNA mismatch repair protein	<i>MLH1</i>	12	3
Ubiquitin hydrolase 10	<i>UBP10</i>	323	35

subunits were identified as Ubp10 unperturbed S phase interactors. Of interest, FACT subunits (Spt16 and Pob3) and RNA pol I subunits (Rpa190, 34, 43, 49 and I35), comprising known functional interactors of Ubp10 Spt16 and Rpa190^{41,48}, were identified with high scores in our proteomic analyzes validating our experimental approach (Supplementary Fig. 1c).

The PCNA-DUB Ubp10 acts downstream of the Fen1^{Rad27} FLAP-endonuclease during DNA replication

Our Ubp10-GFP-Trap proteomic approach shows that Ubp10 interacts physically with major components of the lagging strand synthesis machinery during S phase. Therefore, looking for a functional support of the proteomic evidence, a molecular analysis was designed to reveal a potential role of Ubp10 in the metabolism of OFs. Initially, we focused in discerning the potential interplay of *FEN1* and *UBP10* in the OFM pathway. We had recently shown that Ubp10 and the Fen1 Flap-endonuclease physically interact in early S phase, as detected by co-immunoprecipitation³⁷. To further understand the functional relevance of this observation, we studied genetic interactions occurring in strains ablated for both replication proteins. We first monitored bulk DNA replication in synchronized cell cultures and observed that depletion of Fen1 suppressed the replication defect characteristic of *ubp10* mutants, with *ubp10 fen1* cells showing replication dynamics virtually indistinguishable from that of *fen1* single mutants (Fig. 1a). We then tested fork transitions upon replication stress induction by dNTP pool depletion, in particular by examining the accumulation of anomalous small Ys in *ubp10 Δ* cells³⁷. Small Y-shaped replication intermediates are pathological molecules that accumulate as a consequence of non-canonical transitions from bubbles to large Ys during fork progression upon hydroxyurea (HU)-induced nucleotide depletion in Ubp10 ablated cells. In contrast to single *UBP10* mutants, we found that replication intermediates accumulating in *ubp10 fen1* double mutants are very similar to those of *fen1* single mutant cells and clearly differ from those of *ubp10 Δ* cells, lacking the characteristic

small Y accumulation (Fig. 1b), indicating that Fen1 deletion prevents anomalous nascent strand transitions at stalled forks caused by Ubp10 absence. The functional nature of the genetic interaction was further confirmed by testing thermosensitivity and resistance to chronic exposure to HU, where we found that *fen1 Δ ubp10 Δ* cells phenocopy single *fen1 Δ* mutants (Fig. 1c), indicating that Ubp10 and Fen1 support viability through a single genetically-related pathway and that Fen1 underlies *ubp10 Δ* sensitivity to replication stress. Finally, chromatin fractionation assays in cells synchronously traversing S phase failed to show differences in Fen1 protein accumulation on chromatin in wild-type and *ubp10* defective cells (Fig. 1d), suggesting that Ubp10 does not markedly influence Fen1 chromatin association during OFM. Taken together, these analyzes suggested that absence of the Fen1 endonuclease, required for Okazaki fragment flap-processing, bypasses a yet undefined replication related Ubp10-dependent function.

Ubp10 promotes Okazaki fragment ligation

In order to explore the role of the Ubp10 in lagging strand synthesis, we assayed chromatin binding of key OFM proteins during unperturbed S phase upon Ubp10 depletion. We show a control assay displaying a chromatin fractionation experiment in full (Supplementary Fig. 2), which allows analyzing the partitioning of proteins of interest into chromatin-free and chromatin-bound fractions. For clarity, we only show chromatin-bound fractions in further fractionation assays (including Fig. 1d), unless otherwise stated. PCNA is an abundant protein, detectable throughout the cell cycle, that temporarily associates to chromatin during S phase, in discrete but measurable amounts, in cycles of loading and unloading as the process of DNA synthesis requires^{1,8,26}. Indeed, we observed that PCNA is readily detectable in WCE and chromatin-free fractions, and to a lesser extent on chromatin-bound fractions of cells synchronously undergoing genome replication (Supplementary Fig. 2). Therefore, during replication, a major fraction of PCNA is detectable in soluble forms while a small subset associates to chromatin with a quite reproducible periodicity.

In *S. cerevisiae*, *CDC9* encodes the DNA ligase I, an essential enzyme acting downstream of Fen1 to seal Okazaki fragments during DNA replication^{49,50}. Cdc9 has a human homolog, *LIG1*, also regulated by PCNA during the sealing of nicked DNA at lagging strands⁵¹. Remarkably, human *LIG1* complements yeast *cdc9* temperature-sensitive mutants at the restrictive temperature⁵². Having observed that in budding yeast PCNA-DUB Ubp10 physically interacts with Cdc9 during S phase, we were interested in understanding a possible functional interaction among them.

We studied genetic interactions of *UBP10* with a conditional allele of the DNA ligase I by testing the viability of *cdc9^{ts}* and *ubp10 Δ* double mutant cells. In our study we used a *cdc9-7* allele (from the National BioResource Project, NBRP Japan), a W303 derivative strain that we characterized and sequenced to find that it is synonymous to the *cdc9-1* allele⁵³. We found that depletion of Ubp10 aggravates dramatically the thermosensitivity of strains carrying this *CDC9* temperature-sensitive mutant allele (Fig. 2a). Impaired ligation of Okazaki fragments leads to the accumulation of PCNA on chromatin as a consequence of poor PCNA unloading in the absence of replicative DNA ligase I Cdc9²¹. We observed - by chromatin fractionation assays - that *cdc9-7* cells transiently accumulated PCNA on chromatin when compared to wild-type cells during S phase even under permissive conditions (25 °C) (Fig. 2b). Similarly, under these conditions, *ubp10 Δ* single mutants retained more, and for a longer time, PCNA on chromatin than wild-type cells (Fig. 2b). Furthermore, abrogation of *UBP10* function in the *cdc9-7* mutant cells lead to a significant accumulation of PCNA on chromatin throughout the time-course experiment (Fig. 2b). These observations indicate that the *cdc9-7* allele, likely defective in nick ligation at 25 °C, impairs PCNA unloading, which is largely aggravated by Ubp10 ablation. In fact, the *cdc9-7* mutation did not rescue the

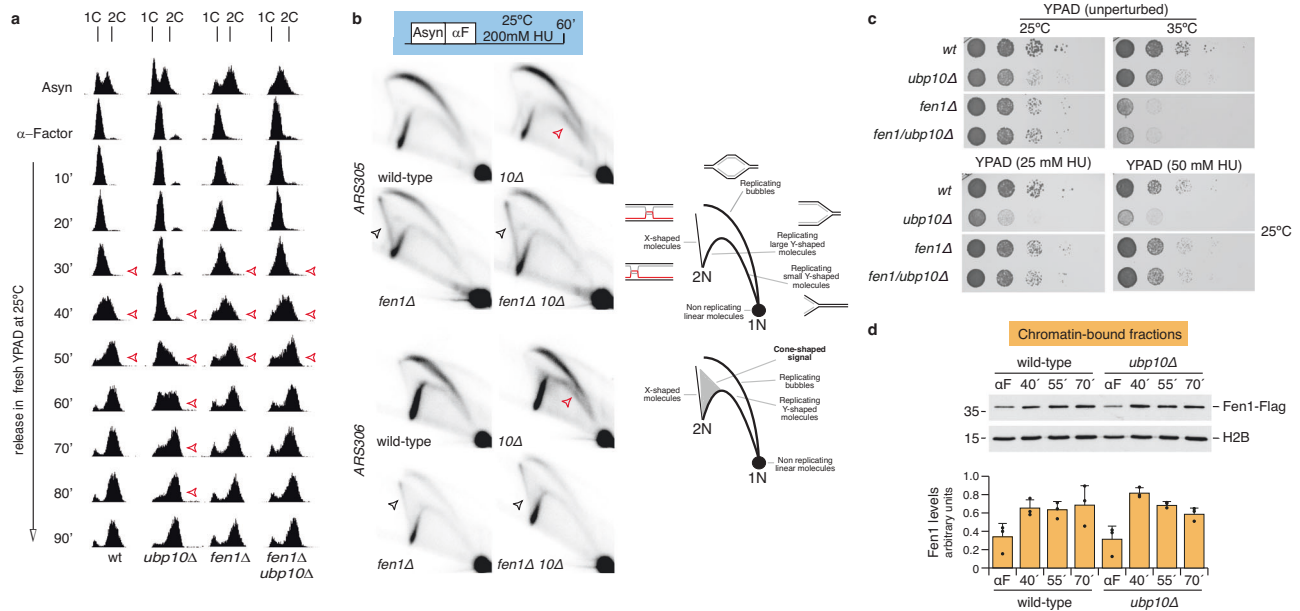


Fig. 1 | Flap-endonuclease *FEN1/RAD27* is epistatic to PCNA-DUB *UBP10* in the Okazaki fragment maturation pathway. **a S phase progression analysis of cells depleted for Fen1 and Ubp10. Wild-type (wt), *ubp10Δ*, *fen1Δ* and *fen1Δ ubp10Δ* exponentially growing were synchronized in G1 with α -factor and release in fresh (rich) media. DNA content by FACS analysis of samples taken at indicated intervals is shown. Red arrows indicate approximated duration of bulk DNA replication for each strain. Note that *fen1Δ ubp10Δ* cells behave like single *fen1Δ* mutants. **b** Cells described in **a** were synchronized with α -Factor and released in the presence of 200 mM HU at 25°C. Samples were taken after 60 min of treatment and processed for 2D-gel analysis of replication intermediates. Membranes were hybridized consecutively with probes spanning *ARS305* and *ARS306* replication origins. Note that *fen1Δ ubp10Δ* cells accumulated X-shaped replication intermediates (black arrows) comparably to *fen1Δ* single mutant cells and in clear contrast to abnormal small Ys intermediates (red arrows) observed in *ubp10Δ* cells (described in Álvarez et al.³⁷). A drawing of the normal replication intermediates and of the abnormal**

intermediates related to DNA replication fork collapse is shown. **c** Ten-fold dilutions of the strains indicated in **a** incubated in YPAD at 25°C or 35°C in the absence (unperturbed) or in the chronic presence of HU (25 mM or 50 mM as indicated). Data presented in **a–c** indicates that *FEN1* is epistatic to *UBP10*. **d** S phase chromatin association of Fen1 in wild-type and *ubp10Δ* cells expressing Fen1-Flag tagged protein. Exponentially growing cultures of wild-type and *ubp10Δ* cells were synchronized with α -factor and released in fresh media to test S phase chromatin association of Flap-endonuclease Fen1/Rad27. Samples were taken at indicated intervals; chromatin-enriched fractions were prepared and electrophoresed in SDS-PAGE gels. Blots were incubated with α -Flag (to detect Fen1-Flag) or α -H2B antibodies. Blots from a representative experiment are shown. Data in the graph represent the average of three biological replicates (and is expressed as means \pm SD in triplicate) ($p = 0.3250$, two-way ANOVA test). This evidence suggests that chromatin association of Fen1 is not affected by depletion of Ubp10. Source data are provided as a Source Data file.

characteristic slow bulk DNA replication phenotype of *ubp10Δ* mutant, but instead further slowed down progression through S phase (Supplementary Fig. 3a, b). We also observed - by 2D-gel analysis of HU-treated cells - that deletion of *UBP10* in *cdc9-7* led to accumulation of unusual replication intermediates to a level equivalent to those observed in *ubp10Δ* single mutants (Supplementary Fig. 3c).

Okazaki fragments can be detected in vivo upon DNA ligase I *CDC9* depletion or using conditional alleles of the ligase, which result in the accumulation of nicked DNA^{49,50}. To test a potential accumulation of Okazaki fragments in *cdc9-7 ubp10Δ* cells and, particularly, after having observed that *cdc9-7* cells grow poorly at 29°C when combined with deletion of *UBP10*, we set up cultures of exponentially growing cells incubated at 25°C to then shifted them to 29°C. Okazaki fragments were end-labeled in samples taken at one-h intervals, separated by denaturing agarose gel electrophoresis, transferred to a nitrocellulose membrane, and visualized with a Phosphor Imager. We detected a transitory accumulation of Okazaki fragments in *cdc9-7* cells upon shifting from 25°C to 29°C degrees cultures of cells growing exponentially. After end-labeling of DNA and denaturing electrophoresis, we observed the characteristic banding pattern of short and heterogenous nicked DNA that results from defects in the ligation at lagging strands⁵⁰ (Fig. 2c). Remarkably, we found that *cdc9-7 ubp10Δ* cells accumulated OFs more abundantly than *cdc9-7* control cells (Fig. 2c). We did not detect this characteristic banding pattern of Okazaki fragments in nick ligation competent wild-type cells or single *ubp10Δ* mutants tested (Supplementary Fig. 3d). In essence, all this evidence indicates that depletion of Ubp10 leads to a strong lagging-

strand replication defect phenotype, downstream of Fen1 function. However, it is important to understand whether this strong phenotype is the cause or the consequence of the slow progression through S phase that characterizes the genetic depletion of Ubp10.

Cells with a defective Flap-endonuclease Fen1/Rad27 accumulate unprocessed Okazaki fragments with poorly ligatable ends due to the accumulation of flaps with different sizes⁵⁴. Furthermore, impairment of PCNA unloader Elg1 function leads to the accretion of extended Okazaki fragments likely reflecting defective post-replicative nucleosome reposition⁵⁵. However, in vivo depletion of Cdc9 DNA ligase I causes the accumulation of nicks that are, therefore, in vitro ligatable with no obvious defects in coupling with chromatin assembly^{50,54}.

To characterize the molecular nature of the Okazaki fragments accumulating in *cdc9-7 ubp10Δ* double mutants, we examined their size by gel electrophoresis and tested the extent to which the isolated DNA fragments are competent for ligation after purification of total DNA. We observed that *cdc9-7 ubp10Δ* cells accumulate Okazaki fragments of normal length (Fig. 2c). In addition, these are ligated in vitro by T4 DNA ligase (Fig. 2d) with an efficiency equivalent to DNA ligase-deficient controls, such as Cdc9-deficient cells^{50,54}. These results indicate that OFs accumulating upon Ubp10 ablation have DNA ends equivalent to those accumulated in *cdc9ts* mutants and suggest that OF accumulation is due to defects in the last steps of lagging strand maturation. The evidence shown so far suggests a role for Ubp10 in the timely maturation of Okazaki fragments, either in the regulation of nick ligation and/or in promoting chromatin disassociation of PCNA.

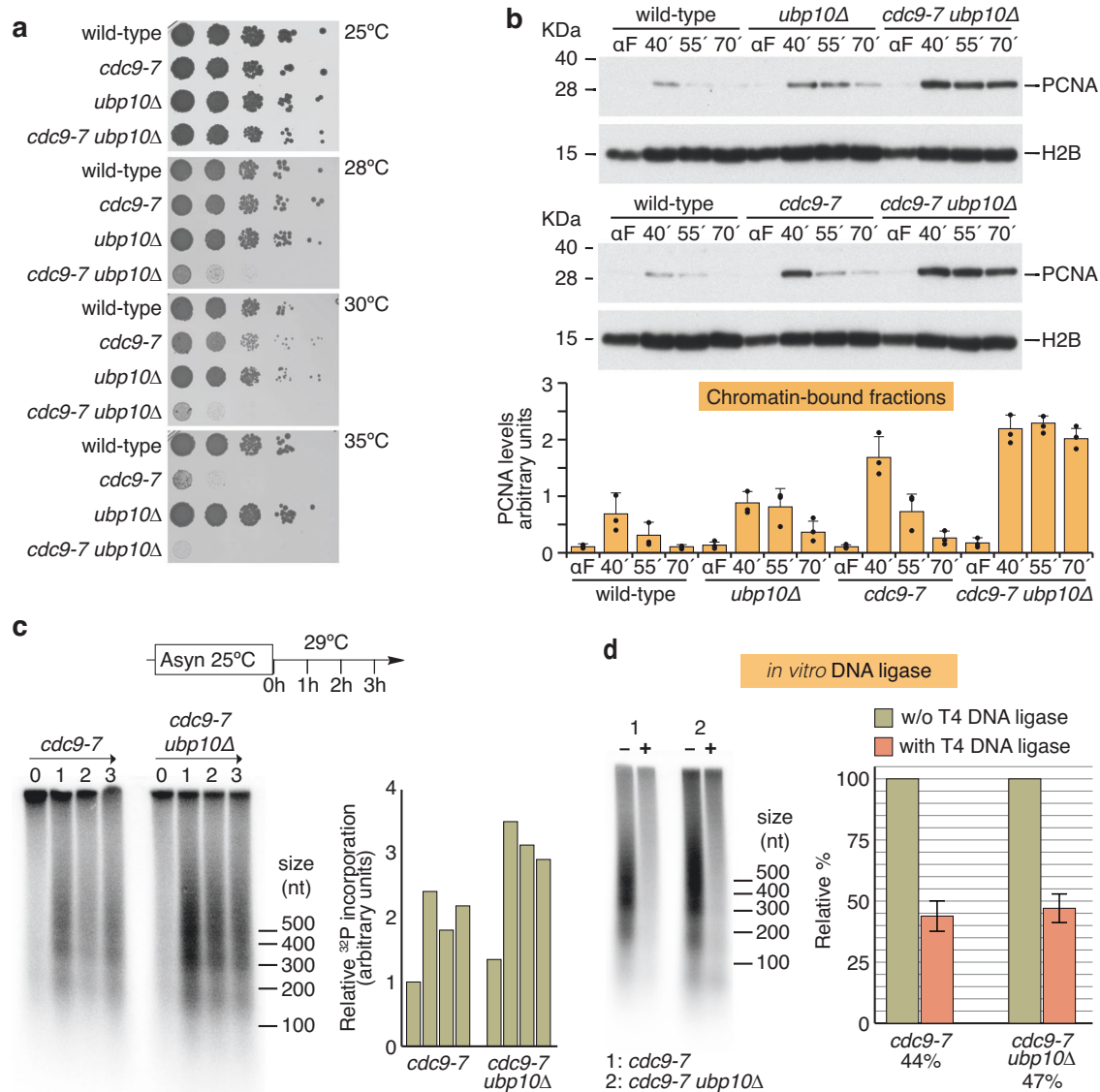


Fig. 2 | Abrogation of Ubp10 leads to accumulation of unligated Okazaki fragments. Depletion of Ubp10 increases the thermosensitivity and PCNA accumulation defects of the *cdc9-7* ts allele of DNA ligase I. **a** Ten-fold dilutions of equal number of cells of the indicated strains were spotted in Petri dishes and incubated either at 25 °C, 28 °C, 30 °C, or 35 °C for 60 h. **b** S phase chromatin association of PCNA in wild-type, *ubp10Δ*, *cdc9-7*, and *cdc9-7 ubp10Δ* cells. Exponentially growing cultures of the indicated strains were synchronized in G1 with α -factor pheromone and released in fresh media to test S phase chromatin association of PCNA. Samples were taken at indicated intervals; chromatin-enriched fractions were prepared and electrophoresed in SDS-PAGE gels. Blots were incubated with α -PCNA or α -H2B antibodies. A blot from a representative experiment is shown. Data in the graph represent the average of three biological replicates (and is expressed as means \pm SD in triplicate) (wild-type vs *ubp10Δ* $p = 0.0482$; wild-type vs *cdc9-7* $p < 0.0006$; wild-type vs *cdc9-7 ubp10Δ* $p < 0.0001$; *ubp10Δ* vs *cdc9-7* $p = 0.3329$; *ubp10Δ* vs *cdc9-7 ubp10Δ* $p < 0.0001$; *cdc9-7* vs *cdc9-7 ubp10Δ* $p < 0.0001$, two-way ANOVA test).

c *UBP10* mutants show a strong detectable lagging-strand replication phenotype that leads to the accumulation of unligated Okazaki fragments (OF). Exponentially growing cultures of *cdc9-7* and *cdc9-7 ubp10Δ* cells incubated at 25 °C were shifted to 29 °C. Aliquot samples were taken at the indicated intervals. Purified total genomic DNA was labeled with exonuclease-deficient DNA polymerase I (Klenow) fragment and α -³²P-dCTP, separated by agarose denaturing electrophoresis, and visualized using a Phosphor Imager. A representative experiment of two biological replicates is shown. The relative amounts of ³²P incorporated by end-labeling was quantitated in a Phosphor Imager and plotted. **d** In vitro analysis of *ubp10Δ* cumulative OFs reveals ligatable nick DNA. OFs were obtained from *cdc9-7* and *cdc9-7 ubp10Δ* cells as in **c**. Where indicated (+) genomic DNA was treated in vitro with T4 DNA ligase before labeling with Klenow and α -³²P-dCTP for quantifying the proportion of DNA fragments (OF) ready for nick ligation. A representative experiment of three replicates is shown. Values of means of these three replicates \pm SD are plotted. Source data are provided as a Source Data file.

Ubp10 is required for timely ligase association to replicating chromatin

PCNA accumulates on replicating chromatin in the absence of Cdc9-mediated Okazaki fragment ligation²¹. We reasoned that the PCNA accretion observed in Cdc9 Ubp10 doubly depleted cells might be the consequence of Cdc9 function defects, due to either impaired DNA ligase activity or to reduced chromatin abundance of Cdc9. Therefore, we next tested a heterologous DNA ligase that can complement Cdc9 depletion⁵⁶, and found that *ubp10Δ* cells overexpressing *Chlorella*

virus DNA ligase exhibit a delay in S phase progression similar to that of controls (Supplementary Fig. 4a), strengthening the conclusion that *ubp10Δ* deficiency is not related with defects in overall DNA ligase activity.

We then monitored Cdc9 chromatin association in synchronously replicating cells and found that Ubp10 depleted cells show transiently reduced ligase levels compared to wild-type cells (Fig. 3), a decrease particularly marked at early time points after G1 release, coinciding with the slow progression of bulk DNA replication and in an inverse

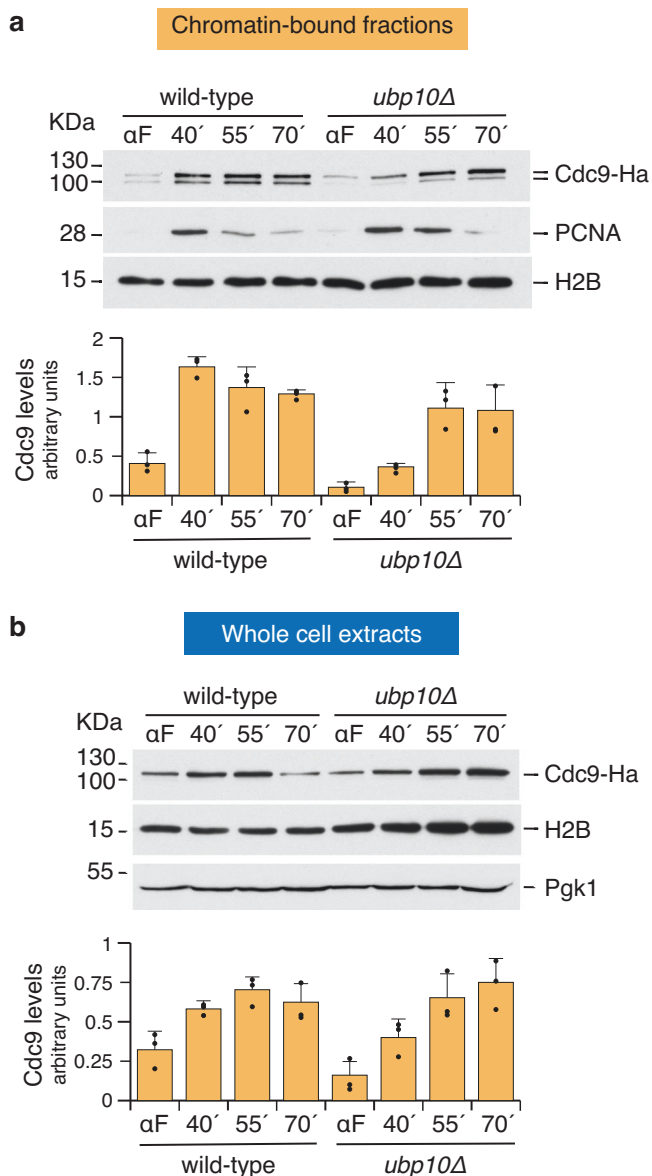


Fig. 3 | Steady reduction of chromatin associated Cdc9 during replication in *UBP10* defective cells. **a** S phase chromatin association of Cdc9 in wild-type and *ubp10Δ* cells. Exponentially growing cultures of wild-type and *ubp10Δ* cells were synchronized with α -factor and released in fresh YPAD media to test S phase chromatin association of DNA ligase I Cdc9. Samples were taken at indicated intervals; chromatin-enriched fractions were prepared and electrophoresed in SDS-PAGE gels. Blots were incubated with α -Ha (to detect Cdc9-Ha), α -PCNA or α -H2B antibodies. A blot from a representative experiment is shown. Data in the graph represent the average of three biological replicates (and is expressed as means \pm SD in triplicate) ($p = 0.0002$, two-way ANOVA test). **b** Whole cell extract (WCE) aliquots from **a** were blotted to test Cdc9-Ha protein amounts. Again, a blot from a representative experiment is shown. Data in the graph represent the average of three biological replicates (and is expressed as means \pm SD in triplicate) ($p = 0.2380$, two-way ANOVA test). Source data are provided as a Source Data file.

correlation with PCNA abundance (Supplementary Fig. 4b,c). Therefore, the accumulation or permanence of PCNA on chromatin in *ubp10Δ* mutants might be the consequence of a slow recruitment of DNA ligase Cdc9 on chromatin. To further understand whether the poor accretion of Cdc9 on chromatin was the cause or a consequence of the slow S phase phenotype of Ubp10 depleted cells, we tested *ubp10Δ* cells overexpressing *CDC9*, by means of a duplicated galactose-inducible allele, and found that high levels of chromatin-

bound Cdc9 did not rescue the characteristic cell cycle defect, lengthy S phase, of *ubp10* mutants nor rescued the accumulation of PCNA (Supplementary Fig. 4b,c). Therefore, we surmise that Ubp10 may directly regulate PCNA unloading from chromatin, indirectly impairing OF ligation.

Increased amounts of ubiquitylated PCNA leads to an increment in chromatin-bound PCNA

We have shown earlier that Ubp12 cooperates with Ubp10 to deubiquitylate PCNA³⁷. Ubp12 depletion does not aggravate *ubp10Δ*-associated slow S phase (ref. 37 and Supplementary Fig. 5a). However, in stark contrast to single mutants, the combined ablation of Ubp10 and Ubp12 accumulates ubiquitylated PCNA both in asynchronous cycling cells³⁷ and during S phase progression (Supplementary Fig. 5b). We then tested the possibility that an increase of ubiquitylated-PCNA in S phase would retain the sliding clamp longer on chromatin and found that, indeed, Ubp10 and Ubp12 depleted cells persistently accumulate chromatin-bound PCNA (Supplementary Fig. 5c), suggesting a link between ubiquitylated PCNA and chromatin retention of the sliding clamp.

Defective deubiquitylation of K164-PCNA underlies the S phase progression defects of Ubp10 depletion

Apart from their roles acting on third substrates, and therefore focusing on nascent DNA, both Ubp10 and Ubp12 limit tolerance events during unperturbed S-phase by reverting ubiquitylation of PCNA at replication forks^{37,57}. Having shown that abrogation of Ubp10 leads to increased levels of chromatin-bound PCNA in S-phase (Fig. 2b) and delays S phase progression (³⁷ and Supplementary Fig. 3a), we tested the hypothesis that deubiquitylation of PCNA-K164 by Ubp10 promotes processive DNA synthesis. For this, we analyzed both phenotypes in *ubp10Δ pol30^{K164R}* double mutant cells and observed that the non-SUMOylable non-ubiquitylable PCNA variant *pol30^{K164R}* suppresses the steady PCNA accumulation as well as the slow progression through S phase that characterize Ubp10 depletion (Fig. 4a, b). This evidence implies that, K164-PCNA is the key target of Ubp10 in S phase and suggests that modification of this Lysine on the sliding clamp plays a main role in unperturbed DNA replication.

As pointed out above, Lysine 164 of the sliding clamp PCNA may be either SUMOylated or ubiquitylated^{27,32}. To discern the importance of SUMO and Ubiquitin modifications, we tested whether overexpression of the Rad18 K164-ubiquitin ligase would mirror the S phase defects conferred by Ubp10 depletion. Indeed, we found that high-levels of Rad18 (opRad18) lead to a slow progression through S phase and a concurrent accumulation of chromatin-bound PCNA equivalent to that observed in *ubp10* cells (Fig. 4c, d). By testing the overexpression of Rad18 in a *pol30^{K164R}* variant background, we also found that both phenotypes depend on ubiquitylation of the K164 residue of PCNA as all opRad18 effects were suppressed by the *K164R* point mutation (Supplementary Fig. 6), in consistence with the previous observation (Fig. 4a, b). All this evidence indicates that dynamic ubiquitylation and deubiquitylation of PCNA at Lysine 164 takes place during unperturbed S phase and plays an important role ensuring processive lagging strand synthesis in yeast.

In the course of these experiments, we noticed that *pol30^{K164R}* mutants of PCNA show reduced accumulation of chromatin-bound PCNA as compared to wild-type cells, somehow suggesting that modification (SUMOylation or ubiquitylation) of this residue may increase the stability of the sliding clamp on chromatin. This *pol30^{K164R}*-associated phenotype is more evident in synchronous S phase (Supplementary Fig. 6) and, particularly, when synchronized cultures are incubated in galactose-based media, circumstance where yeast cells slow progression through S phase (Supplementary Fig. 6). A reduced stability of the sliding clamp in replicating DNA may explain the faulty processing of Okazaki fragments detected in vitro in DNA replication assays based on the use of yeast PCNA-K164R⁴⁷.

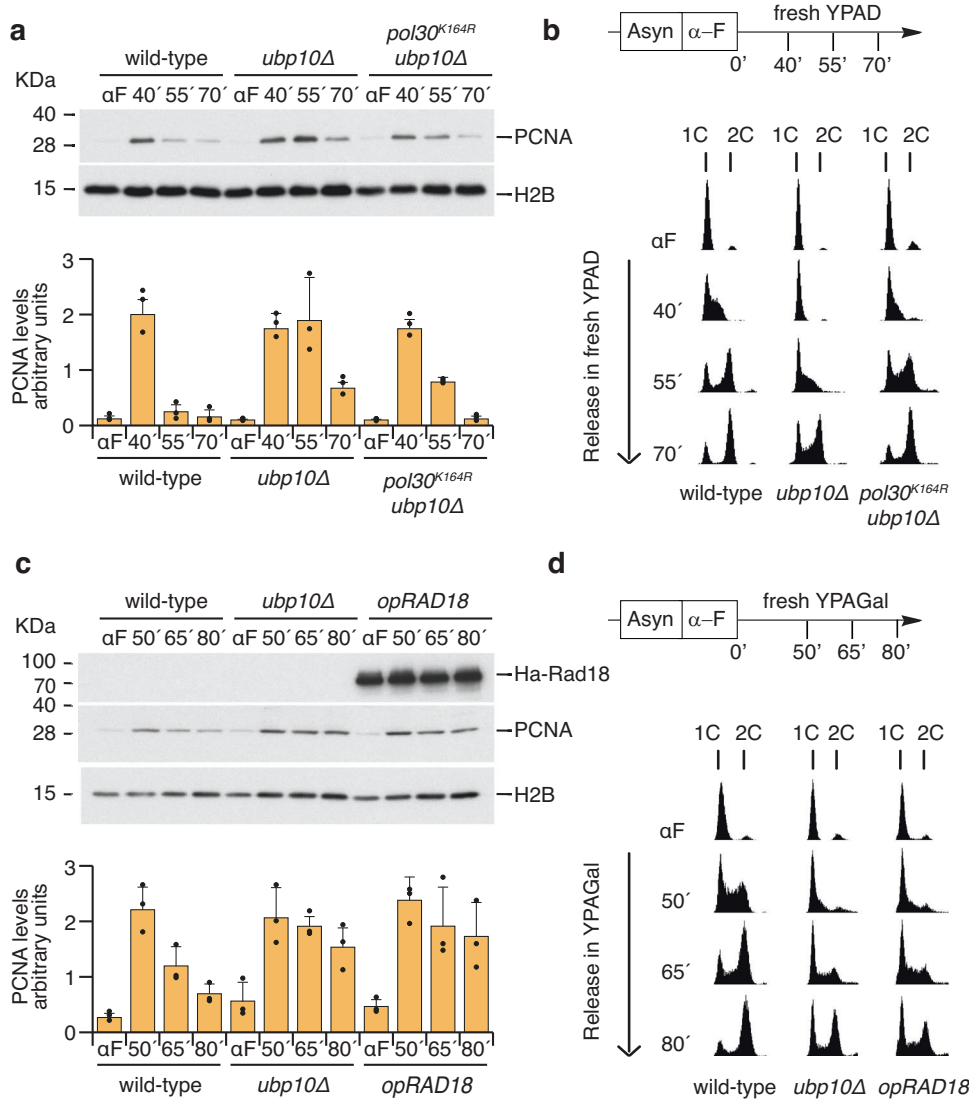


Fig. 4 | Processive S phase progression is ensured by dynamic ubiquitylation and deubiquitylation of PCNA Lysine 164. **a** S phase chromatin association of PCNA in wild-type, *ubp10Δ* and *ubp10Δ pol30^{K164R}* cells. Exponentially growing cultures of wild-type, *ubp10Δ* and *ubp10Δ pol30^{K164R}* cells were synchronized in G1 with the α -factor pheromone and released in fresh (glucose-based) media to test S phase chromatin association of PCNA. Samples were taken at indicated intervals; chromatin-enriched fractions were prepared and electrophoresed in SDS-PAGE gels. Blots were incubated with α -PCNA or α -H2B antibodies. A blot from a representative experiment is shown. Data in the graph represent the average of three biological replicates (and is expressed as means \pm SD in triplicate) (wild-type vs *ubp10Δ* $p = 0.0003$; wild-type vs *ubp10Δ pol30^{K164R}* $p = 0.8376$; *ubp10Δ* vs *ubp10Δ pol30^{K164R}* $p = 0.0011$, two-way ANOVA test). **b** The characteristic *ubp10Δ* slow S phase progression is suppressed by non-ubiquitylable PCNA^{K164R} variant form. DNA content analysis by FACS of wild-type, *ubp10Δ*, and *ubp10Δ ubp12Δ* cells at the indicated time points (aliquot samples of the experiment in **a**). **c** Overexpression of

the K164-ubiquitin ligase Rad18 leads to chromatin PCNA accumulation and a slow progression through S phase. S phase chromatin association of PCNA in wild-type, *ubp10Δ* and *GALI-10:RAD18 (opRAD18)* cells. Exponentially growing cultures of the indicated strains incubated in YPAGalactose were synchronized in G1 with the α -factor pheromone and released in fresh (galactose-based) media to test S phase chromatin association of PCNA. Samples were taken at indicated intervals; chromatin-enriched fractions were prepared and electrophoresed in SDS-PAGE gels. Blots were incubated with α -PCNA or α -H2B antibodies. A blot from a representative experiment is shown. Data in the graph represent the average of three biological replicates (and is expressed as means \pm SD in triplicate) (wild-type vs *ubp10Δ* $p = 0.0457$; wild-type vs *opRAD18* $p = 0.0096$; *ubp10Δ* vs *opRAD18* $p = 0.7701$, two-way ANOVA test). **d** DNA content analysis by FACS of wild-type, *ubp10Δ*, and *opRAD18* cells at the indicated time points (aliquot samples of the experiment in **c**). Source data are provided as a Source Data file.

PCNA disassembly-prone mutants *pol30^{R14E}* and *pol30^{D150E}* revert *ubp10Δ*-associated replication defects

We reasoned that the excessive abundance of PCNA on chromatin in *Ubp10* depleted cells might be related to defective unloading of the sliding clamp. If *ubp10Δ* phenotypes are related with the excessive retention of PCNA on chromatin, two predictions can be made. Firstly, cells depleted for *Ubp10* should accumulate PCNA on chromatin during S phase. Secondly, a reduction in the amount of PCNA bound to chromatin would rescue *ubp10* replication defects. Regarding this second prediction, there are a number of *POL30* alleles that conform unstable

PCNA homotrimers⁵⁸. In particular, *pol30^{R14E}* and *pol30^{D150E}* alleles are described as PCNA trimer-disassembly-prone mutants due to their instability when bound to chromatin^{21,58}. Hence, if the reason underlying *ubp10* defects is related to excessive PCNA on chromatin, the potential suppression by these disassembly-prone PCNA mutants might be easier to observe in a *cdc9-7 ubp10Δ* background due to the greater thermosensitivity as compared to single *cdc9-7* cells. In fact, the growth defect of *cdc9-7 ubp10Δ* is suppressed by *pol30^{R14E}* and *pol30^{D150E}* mutant alleles, while they did not rescue *cdc9-7* thermosensitivity (Fig. 5a). Furthermore, these point mutant alleles of PCNA also rescue abnormal replication

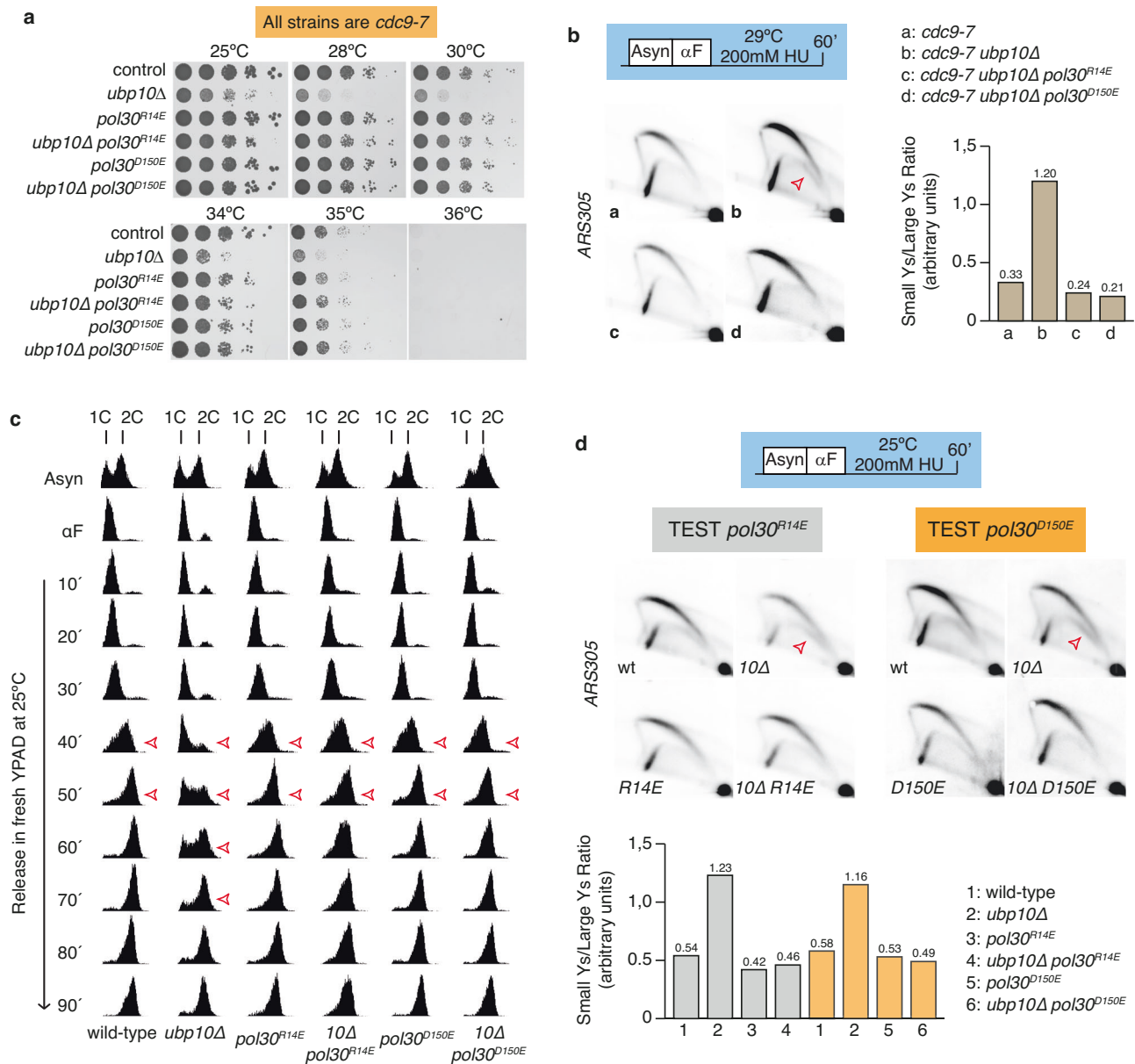


Fig. 5 | PCNA disassembly-prone mutants *pol30^{R14E}* and *pol30^{D150E}* revert *ubp10Δ*-associated replication defects. **a *pol30^{R14E}* and *pol30^{D150E}* alleles rescue *ubp10Δ*-associated defects in *cdc9-7 ubp10Δ*. Ten-fold dilutions of the *cdc9-7* indicated strains incubated in YPAD at different temperatures for 60 h. Note that the increased lethality of *cdc9-7 ubp10Δ* is suppressed by *pol30* mutant alleles that, in turn, do not rescue *cdc9-7* thermosensitivity. **b** 2D-gel analysis of cells synchronized in early S phase with the ribonucleotide reductase inhibitor HU at 29°C. Indicated *cdc9-7* strains were grown to exponential phase at 25°C, synchronized in G1 with α -factor, released in fresh media with 200 mM HU at 29°C for 60 additional min. The membrane was hybridized to a probe spanning *ARS305* early replication origin. Open red arrow points small Ys intermediates. Under these conditions, *cdc9-7 ubp10Δ* defects were suppressed by PCNA disassembly-prone mutants. Histogram plots of small/large Y-shaped replication intermediates ratios in *cdc9-7*, *cdc9-7 ubp10Δ*, *cdc9-7 ubp10Δ pol30^{R14E}* and *cdc9-7 ubp10Δ pol30^{D150E}* mutants are shown. **c** DNA replication progression defects in *ubp10Δ* cells are abrogated by *pol30^{R14E}***

and *pol30^{D150E}* alleles. DNA content analysis of wild-type, *ubp10Δ*, *pol30^{R14E}*, *ubp10Δ pol30^{R14E}*, *pol30^{D150E}* and *ubp10Δ pol30^{D150E}* strains. Cells of the indicated strains (all *cdc9td* with *CDC9 ON*) were synchronized with α -factor and released in fresh YPAD at 25°C. The progression of the bulk genome replication was monitored at the indicated time points. Open red arrows indicate approximate S phase duration in every strain where *pol30^{R14E}* and *pol30^{D150E}* suppression of the replication defect of *ubp10Δ* cells can be observed. **d** 2D-gel analysis of replication intermediates in cells synchronized in early S phase with HU. Indicated strains grown to exponential phase at 25°C were pre-synchronized in G1 with α -factor, released in fresh media with 200 mM HU and incubated at the same temperature for one additional hour. Membranes were hybridized to a probe spanning *ARS305* early replication origin. Open red arrows indicate small Ys intermediates in blots. Histogram plots of small/large Y-shaped replication intermediates ratios in wild-type and *ubp10Δ*, *pol30^{R14E}*, *ubp10Δ pol30^{R14E}*, *pol30^{D150E}* and *ubp10Δ pol30^{D150E}* mutants are shown. Source data are provided as a Source Data file.

intermediates accumulated in *cdc9-7 ubp10Δ* cells arrested in HU (Fig. 5b). In fact, these *POL30* alleles rescue all tested Ubp10-depletion associated S phase defects, including those related with bulk genomic DNA replication in a *CDC9* wild-type-like strain (Fig. 5c), implying that the slow S phase observed in Ubp10 depleted cells is directly linked to PCNA accumulation on replicating chromatin. Reduced replication

intermediate levels in HU-treated *UBP10* deleted cells were also efficiently suppressed by either *pol30^{R14E}* or *pol30^{D150E}* (Fig. 5d). This evidence links the replication phenotypes caused by Ubp10 ablation to a defective PCNA unloading mechanism during S phase.

UBP10 mutants accumulate non-canonical small Y-shaped replication intermediates upon HU-induced fork stalling³⁷. The

accumulation of these non-canonical small Ys is characterized by a decrease in large Ys and is abated by mutating *RADS2*³⁷. We re-examined the accumulation of these small Y-shaped molecules and found that is suppressed in *pol30^{RI4E}* and *pol30^{DISOE}* genetic backgrounds (Fig. 5b, d). These results strongly suggest that small Y-shaped molecules formed downstream of Fen1 function as a direct consequence of PCNA accumulation on replicating chromatin and, also, that these abnormal structures are generated as cells try to repair through a Rad52-dependent TS-like mechanism.

The disassembly-prone mutant *pol30^{DISOE}* suppresses increased chromatin association of PCNA and OF accumulation in *UBP10* defective cells

As mentioned, if *ubp10* phenotypes are the consequence of a defective unloading of PCNA, cells depleted for Ubp10 should accumulate the sliding clamp on chromatin during S phase, indeed we have observed a chromatin-bound accretion of PCNA in *ubp10Δ* cells when testing *cdc9-7* mutants and Cdc9 levels (Figs. 2b, 3a, 4a, c, and Supplementary Figs. 4c, 5c). We next re-evaluated how much and for how long the sliding clamp PCNA is bound to chromatin through a synchronized, otherwise unperturbed, S phase in wild-type and *ubp10Δ* cells. As expected from previous results (Fig. 5c), we found that the slow S phase progression in *ubp10Δ* cells correlates with an increased PCNA accumulation on chromatin (Fig. 6a, b). In parallel, we also evaluated the disassembly-prone *pol30^{DISOE}* point-mutant ability to suppress this chromatin-bound PCNA accretion phenotype and found that this PCNA mutant rescued chromatin retention of PCNA of *ubp10Δ* (Fig. 6a, Supplementary Fig. 7), as well as the bulk DNA replication defect (Fig. 5c).

Having shown that PCNA accumulation on replicating chromatin underlies not only the slow S phase progression but also the formation of anomalous small Ys in *ubp10* defective cells, we next tested whether the PCNA disassembly-prone *pol30^{DISOE}* allele would be able to rescue the accumulation of unligated Okazaki fragments that can be evidenced in the *ubp10* mutant using a *cdc9-7* background. It has been shown that *pol30^{RI4E}* and *pol30^{DISOE}* PCNA trimer-disassembly-prone mutants alleviate the Okazaki fragment length extension problem described in *elg1Δ* cells⁵⁵, in agreement with PCNA unloading being a key event in maturation of the lagging strand and nucleosome deposition. We predicted that *pol30^{DISOE}* would mitigate the OF accretion of *cdc9-7 ubp10Δ* cells. To test this hypothesis, exponentially growing *cdc9-7*, *cdc9-7 ubp10Δ*, *cdc9-7 pol30^{DISOE}* and *cdc9-7 pol30^{DISOE} ubp10Δ* cells incubated at 25 °C were shifted to 29 °C, and samples were taken at one-hour intervals and processed for OF analysis. We observed that the *pol30^{DISOE}* point mutant suppresses *ubp10Δ* Okazaki fragment maturation timing defect (Fig. 6c), implying that the main problem caused by Ubp10 depletion during lagging strand replication is caused by PCNA retention on chromatin.

Ubp10 as a key regulator of a PCNA unloading mechanism likely distinct from Elg1-RLC

Thus far, our results argue that Ubp10 promotes timely PCNA unloading during lagging strand replication. One reasonable hypothesis is that Ubp10 promotes PCNA deubiquitylation to enhance Elg1-mediated PCNA unloading at the final steps of Okazaki fragment maturation. Fully aware of in vitro evidence showing that human ATAD5^{Elg1} is able to unload both ubiquitylated and deubiquitylated PCNA forms with similar efficiency⁵⁹, we reasoned that in vivo, during unperturbed DNA replication, chromatin PCNA unloading would be enhanced by deubiquitylated forms of the sliding clamp in order to proceed smoothly and timely through lagging strand synthesis.

Yeast Elg1^{ATAD5} is an evolutionary conserved homolog of the replication factor C (RFC) subunit Rfc1^{23,25}. It has been shown that while Rfc1-RFC loads PCNA on replicating chromatin, the Elg1-RLC complex has a role in PCNA unloading in a molecular event preceded by Okazaki

fragment ligation^{18,21}. Elg1 forms an alternative RFC hetero-pentameric complex with all RFC2-5 subunits of RFC. Significantly, this alternative Elg1-RLC complex is important but not essential for DNA replication²⁴. Elg1 interacts physically with PCNA and Fen1^{Rad27}, has a role in PCNA unloading during Okazaki fragment maturation and is, therefore, important for efficient S phase progression, and likely has a role in proper nucleosome assembly^{18,25,55}.

We have observed that, though Elg1 displays many phenotypes related to chromosome stability, depletion of *ELG1* in budding yeast do not cause major replication delays as assayed in synchronous S phase (Supplementary Fig. 8a). In fact, bulk DNA replication timing in *ELG1* mutants is equivalent to wild-type replication as tested by FACS DNA content analysis (Supplementary Fig. 8a). Moreover, deletion of *ELG1* is viable while deletion of other RFC components is not (in particular RFC1)^{24,26}. However, in 10-fold dilution assays we detected that *elg1Δ* strains show a poor growth rate particularly at high temperatures (Supplementary Fig. 8b). A defect exacerbated when single *elg1Δ* mutation is combined with the deletion of Ubp10 (*ubp10Δ elg1Δ*) at any tested temperature, as compared to single mutants or wild-type cells (Supplementary Fig. 8b). This semi-lethality is indicative of a genetic interaction suggestive of a role for both factors in a common event, likely PCNA unloading.

To test chromatin-bound PCNA levels throughout S phase in wild-type, double mutant *elg1Δ ubp10Δ*, and single mutants *elg1Δ* and *ubp10Δ*, mid-log phase cultures of the indicated strains were synchronized in G1 with α -factor and released in fresh media. As in previous experiments, samples were taken at indicated time points and processed for chromatin pellet assays and DNA content analysis (Fig. 7). We initially expected *elg1Δ ubp10Δ* double mutants to behave like *elg1Δ* singles in accordance with the hypothesis that Ubp10 might regulate PCNA unloading through Elg1. Unexpectedly, we found that *ubp10Δ* and *elg1Δ*, when combined, are additive regarding PCNA accumulation on replicating chromatin (Fig. 7a, b), suggesting the existence of two parallel pathways of PCNA unloading. The simplest explanation for these observations is the existence of a PCNA chromatin disassociation mechanism regulated by Ubp10 separable from the Elg1^{ATAD5}-dependent unloading.

Even though the proteomic analysis presented in this work revealed no interaction with the RFC cofactor Elg1, we examined whether the ablation of Ubp10 altered the chromatin binding pattern of Elg1 during a synchronized S phase. By chromatin fractionation assays, we found that depletion of the PCNA-DUB does not alter Elg1 interaction with chromatin (Supplementary Fig. 8c). Therefore, we concluded that *UBP10* mutants do not deregulate Elg1 interaction with chromatin during S phase. Significantly, cells depleted for both *UBP10* and *ELG1* do not exacerbate the slow S phase phenotype conferred by *ubp10Δ* deletion (Fig. 7c), though they accumulate PCNA abundantly, far more than individual mutants (Fig. 7a, b). The fact that depletion of *UBP10* alone has a replication progression defect underpins the importance of this Ubp10-dependent PCNA unloading mechanism for lagging strand synthesis.

Discussion

Okazaki fragment maturation is a complex, yet well understood, process in the synthesis of the lagging strand during DNA replication. Here, we unveil a role of the ubiquitin protease Ubp10 in the latest steps of maturation of Okazaki fragments in the model yeast *S. cerevisiae*. In yeast, the Ubp10 enzyme has been functionally related to RNA polymerase I through the stabilization of the Rpa190 subunit⁴¹. Ubp10 also cooperates with the FACT complex in the maturation of nucleosomes⁴⁸. Furthermore, Ubp10 is involved in the reversal of histone H2B^{K123} ubiquitylation³⁸⁻⁴⁰. Significantly for this report, a key role of this deubiquitylase is to counteract futile bypass events at replication forks acting as a PCNA^{K164}-DUB³⁷. PCNA deubiquitylation is a requirement conserved throughout evolution as evidence for

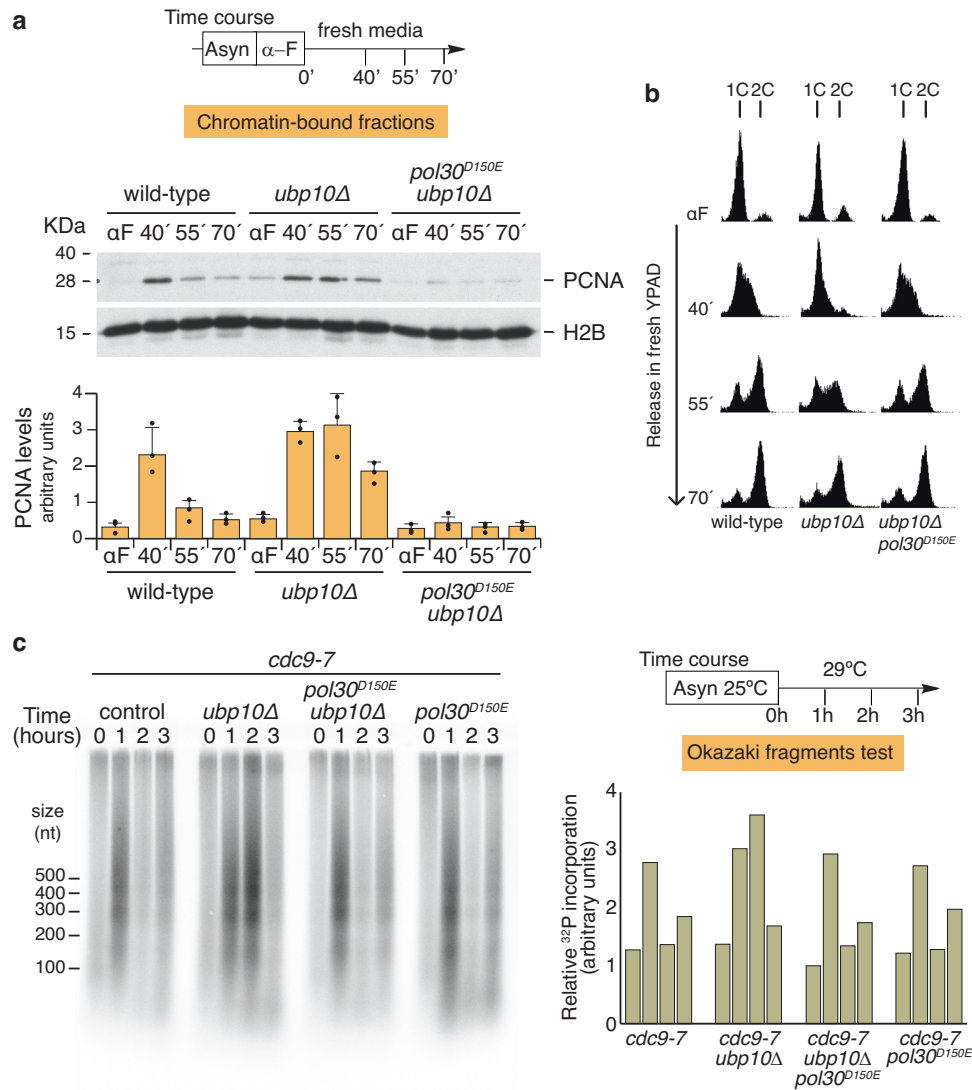


Fig. 6 | PCNA retention on replicating chromatin underlies Okazaki fragments accumulation in Ubp10 abrogated cells. **a** PCNA trimer-disassembly-prone mutant *pol30*^{D150E} suppresses PCNA retention on chromatin phenotype of Ubp10 depleted cells. Exponentially growing cultures of wild-type, *ubp10* Δ , and *pol30*^{D150E} *ubp10* Δ cells were synchronized in G1 with α -factor and released in fresh media to test S phase chromatin association of PCNA. Samples were taken at indicated intervals; chromatin-enriched fractions were prepared and electrophoresed in SDS-PAGE gels. Blots were incubated with α -PCNA or α -H2B antibodies. A blot from a representative experiment is shown. Data in the graph represent the average of three biological replicates (and is expressed as means \pm SD in triplicate) (wild-type vs *ubp10* Δ $p < 0.0001$; wild-type vs *pol30*^{D150E} *ubp10* Δ $p < 0.0004$; *ubp10* Δ vs *pol30*^{D150E} *ubp10* Δ $p < 0.0001$, two-way ANOVA test). **b** Slow S phase progression in

PCNA-DUB *UBP10* defective cells is a direct consequence of PCNA accumulation on replicating chromatin. DNA content analysis of wild-type, *ubp10* Δ , and *pol30*^{D150E} *ubp10* Δ cells at the indicated time points (aliquot samples of the experiment in **a**). **c** *pol30*^{D150E} rescues *ubp10* Δ Okazaki fragments maturation timing defects. Exponentially growing cultures of *cdc9-7*, *cdc9-7 ubp10* Δ , *cdc9-7 pol30*^{D150E} and *cdc9-7 pol30*^{D150E} *ubp10* Δ cells incubated at 25°C were shifted to 29°C. Aliquot samples were taken at the indicated one-hour intervals. Purified total genomic DNA was labeled with exonuclease-deficient DNA polymerase I, Klenow fragment and α -³²P-dCTP, separated by agarose denaturing electrophoresis, and visualized using a Phosphor Imager. A representative experiment of two biological replicates is shown. Relative ³²P incorporation by end-labeling in the Okazaki fragment test was quantitated and plotted. Source data are provided as a Source Data file.

ScUbp10, SpUbp16 and HsUsp1 shows^{36,43}. With this background in mind, the aim of this work was to understand the functional meaning of the interaction of the PCNA-DUB Ubp10 with proteins involved in Okazaki fragment synthesis and maturation, physical interaction described earlier for the Flap endonuclease Fen1^{Rad27,37}. In this study we have presented ample evidence suggesting that this DUB regulates the dissociation of the sliding clamp PCNA from chromatin and that, by doing so, ensures proper maturation of the lagging strand.

One recent observation, Fen1^{Rad27}-Ubp10 binding³⁷, led us to the study of Ubp10's S phase proteome. The analysis confirmed previous data regarding Ubp10 biology as the RNA polymerase I complex subunits Rpa190, Rpa34, Rpa43, Rpa49 and Rpa135 were among proteins trap with Ubp10. Spt16 and Pob3 FACT subunits were also found to bind Ubp10-

GFP. Our approach confirmed Fen1-Ubp10 and PCNA-Ubp10 interactions and identified major components of synthesis and maturation of the lagging strand as feasible interactors of the PCNA-DUB. The proteomic studies were made in crosslinked protein samples from cells synchronized in S phase. We confirmed each observed interaction by individually testing Ubp10 ability to form a complex with each OFM complex component of interest in tagged strains during S phase.

A relevant point for this work is understanding the nature of the cell cycle defect of Ubp10 depleted cells, a defect we believed is poorly understood^{36,37,41,42}. Growth and cell cycle defects are separable^{37,42}. In our studies, we did not observe a G1 delay defect^{36,37}. Further, the timing of entry into S phase is close to that of the wild-type, with equivalent timing in ARSs activation³⁷. *ubp10* Δ characterization

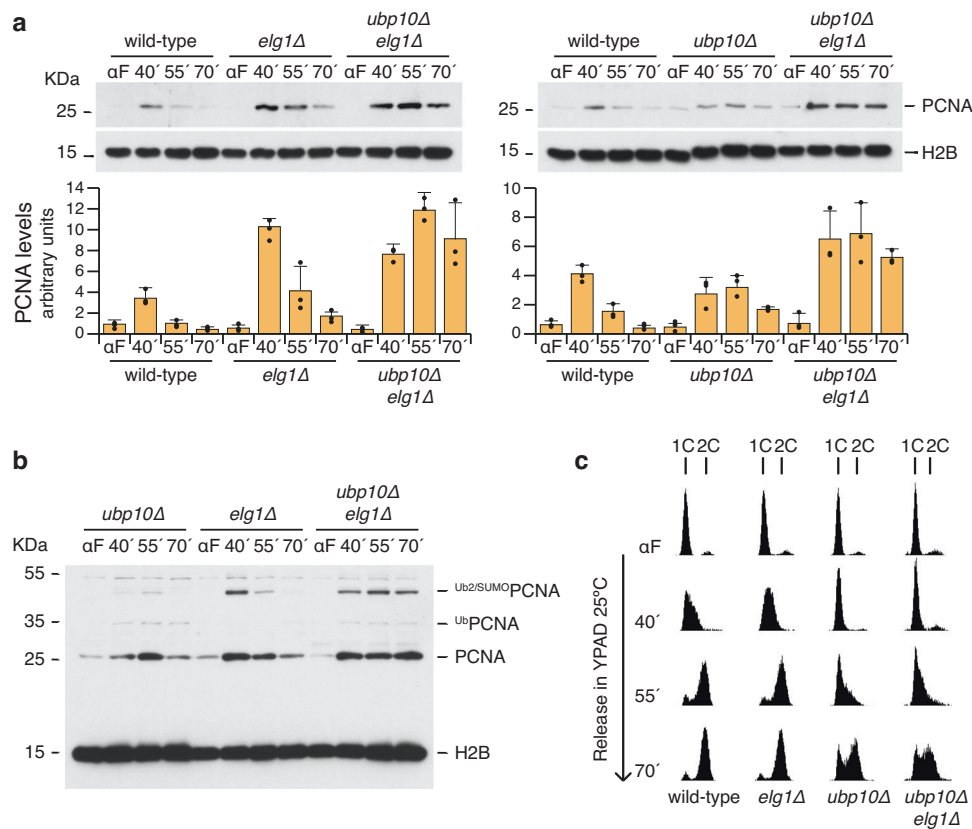


Fig. 7 | Ubp10 is a key regulator of a PCNA unloading mechanism likely distinct from Elg1-RLC. **a** Abrogation of Ubp10 is strongly additive to Elg1 depletion resulting in substantial increase of PCNA bound to chromatin during replication. S phase chromatin association of PCNA in wild-type, *elg1Δ*, *ubp10Δ* and *elg1Δ ubp10Δ* cells. Exponentially growing cultures of the indicated strains were synchronized in G1 with α -factor and released in fresh media to test S phase chromatin association of PCNA and histone H2B. Samples were taken at indicated intervals; chromatin-enriched fractions were prepared and electrophoresed in SDS-PAGE gels. Blots were incubated with α -PCNA or α -H2B antibodies. Blots from representative experiments are shown. Data in the graphs represent the average of three biological replicates (and are expressed as means \pm SD in triplicate) (wild-type vs *elg1Δ*

$p < 0.0001$; wild-type vs *ubp10Δ elg1Δ* $p < 0.0001$; *elg1Δ* vs *ubp10Δ elg1Δ* $p < 0.0001$, two-way ANOVA test). Note that depletion of Elg1 results in transient accumulation of PCNA on chromatin during S phase. **b** S phase chromatin association of PCNA and histone H2B in *ubp10Δ*, *elg1Δ* and *elg1Δ ubp10Δ* cells. The samples correspond to technical replicates of some of the samples shown in **a**, resolved in the same gel to better compare transient accumulation of PCNA (as well as SUMOylated-, and Ubiquitylated-PCNA modified forms) on replicating chromatin in *ubp10Δ* and *elg1Δ* single mutants in the same blot. **c** S phase progression analysis of wild-type, *elg1Δ*, *ubp10Δ* and *elg1Δ ubp10Δ* cells. Progression of bulk genome replication was monitored at the indicated time points by FACS analysis. Source data are provided as a Source Data file.

indicates that the defective cell cycle is a consequence of the slow-down in DNA replication progression. We also found here that this defect is based on the accretion of chromatin-bound PCNA during S phase and that, consistent with this evidence, it is efficiently suppressed by PCNA-disassembly-prone *pol30^{R14E}* and *pol30^{D150E}* mutant alleles (see below).

Fission yeast cells increase the amount of chromatin-associated PCNA when the K164 of this sliding clamp is ubiquitylated⁴⁴. Based on their observations, Daigaku and coworkers proposed that in *S. pombe* an increase in Ub-PCNA^{K164} works to expand the time for PCNA-Pol δ binding to chromatin to allow the completion of OFs. Our findings in *S. cerevisiae* are consistent with a scenario where ubiquitylation of PCNA is a DNA retention signal for the sliding clamp at lagging strands in unperturbed replication. Indeed, the analysis of the rescue of the defective S phase parameters of Ubp10 depletion or Rad18 overexpression by *pol30^{K164R}*, non-ubiquitylatable point mutant of PCNA, proves that dynamic ubiquitylation and deubiquitylation of the Lysine 164 of the sliding clamp is a relevant event in PCNA unloading that ensures timely progression through S phase. In a cause-and-effect link (further discussed below), the increase in chromatin-bound PCNA likely slows down progression through S phase in budding yeast. This is consistent with previous evidence in *S. pombe* cells, where depletion of PCNA-DUBs leads to a cell cycle

delay phenotype suppressed by abrogation of the PCNA-ubiquitin-ligase Rhp18⁴³.

HsUsp1 in human cells, SpUbp16 in fission yeast *S. pombe*, and ScUbp10 in *S. cerevisiae* are orthologous genes that revert PCNA ubiquitylation^{33,37,43}. Therefore, it can be expected that HsUsp1 and SpUbp16 might perform a similar role during lagging strand synthesis, as described here for ScUbp10, given that PCNA is also dynamically ubiquitylated and deubiquitylated during S phase in humans and fission yeast.

Of particular interest for our work were both the study of the cell cycle defect of Ubp10 depleted cells and the analysis of the genetic interactions that arise from individual mutants in the OFM pathway when combined with *ubp10Δ*. One of these analyses has been made in a Cdc9 defective background. In this analysis, not only we found a semi-synthetic lethality among *cdc9-7* and *ubp10Δ* but also created a tool and found a temperature for the OF accumulation tests. Indeed, *cdc9-7 ubp10Δ* results suggest that ablation of the PCNA-DUB Ubp10 leads to a strong lagging-strand replication defect phenotype, possibly owing to defects in Okazaki fragment ligation. On the other hand, we also show that the slow S-phase or OF accumulation phenotypes in *ubp10Δ* are unrelated to Cdc9 presence or activity. Therefore, we surmise that *ubp10Δ* cells have a genuine defect in the maturation of Okazaki fragments related to PCNA unloading.

We have performed a series of experiments to measure the length and molecular nature of the abundant OF accumulated in *UBP10* mutant cells and, in summary, all observations indicate that only abundance is affected. Regarding the length, the detected OF in *cdc9-7 ubp10Δ* cells displayed the distinctive size periodicity evocative of the nucleosome repeat length and were very similar to those observed for *cdc9-7*. Moreover, we show here that Ubp10 accumulated OF are in vitro ligatable to the same extent as controls (*cdc9-7 ubp10Δ* versus *cdc9-7*), and controls are in accordance with published data⁵⁴ again indicating that OFs are conventional nicked DNA. Since it has been demonstrated that lagging-strand synthesis in budding yeast is coupled with chromatin assembly on newly synthesized DNA⁴⁰ we deduce as well that chromatin assembly is not affected in Ubp10 depleted cells.

Smith and Whitehouse have shown that *rad9Δ* and *tof1Δ* checkpoint mutants when combined with a *cdc9^{td}*-degron allele accumulate abundant but normal length Okazaki fragments when *Cdc9^{td}* is proteolyzed⁵⁰. This observation is particularly strong, in terms of OF abundance, for *tof1Δ* mutants and is relevant for our work given the similarity with *ubp10Δ* data presented here. There is not such a strong accumulation in *cdc9^{td} rad9Δ* case⁵⁰. Tof1, named after topoisomerase I-interacting factor, is pertinent to this work because is a subunit of the Csm3-Mrc1-Tof1 replication pausing-mediator complex functionally associated with DNA replication forks⁶⁰⁻⁶³. On the other hand, the N-terminus of FACT-subunit Spt16 interacts with Tof1 to ensure chromatin replication in vitro⁶⁴, supporting the hypothesis that FACT is recruited to replication forks by the Tof1-fork replication complex for parental nucleosomes removal. Given that the FACT complex interacts with Ubp10 likely to integrate transcription and DNA replication with nucleosome assembly⁴⁸, a complex Tof1-FACT-Ubp10 connection emerges likely involved in robust DNA replication progression.

As mentioned before, an important conclusion here is that *ubp10Δ* S phase defects do not involve direct regulation of *Cdc9* function. However, we observed that *ubp10Δ* cell cycle deficiency was assumably a consequence of increased residence time of PCNA during S phase and was directly related with a defective unloading of the sliding clamp in Ubp10 depleted cells. Accordingly, disassembly-prone mutant alleles of *POL30*, *pol30^{R14E}* and *pol30^{D150E}*, rescue *ubp10Δ* mutant defects. A corollary of these two remarkable observations is that during unperturbed S phase PCNA unloading may occur simultaneously with or even before *Cdc9*-mediated nick ligation and this may be in contrast with evidence published regarding Elg1 in the PCNA unloading subject²¹. However, this is a preliminary observation, and therefore, further work would be required to understand this conundrum.

Our observations do not exclude a functional interaction between Ubp10 and *Cdc9* during OFM, as chromatin-bound *Cdc9* levels remain low in Ubp10-ablated cells even when the rest of the cell cycle phenotypes are suppressed in PCNA disassembly-prone mutants. However, our results do not favor the hypothesis that *Cdc9* loading defects underlie *ubp10Δ*-associated cell cycle phenotypes, as we have found that deubiquitylation of the Lysine 164 of PCNA is the relevant event in Ubp10-mediated PCNA unloading that ensures timely progression through S phase.

Besides the slowdown in replication progression, the ablation of Ubp10 is characterized by the accumulation of non-canonical replication intermediates in HU-treated cells detected as small Ys by 2D-gel analysis. These intermediates are observed upon Ubp10-DUB depletion, suggesting that they are normally suppressed by PCNA deubiquitylation³⁷. Canonical small Ys reflect passive replication by forks arising outside the probed fragment. We suggest that accumulation of small Ys may also reflect pathological features of lagging strand-associated replication fork defects (nick DNA that may generate breakage structures, following Fen1-mediated flap cleavage). Special consideration should be given to replication intermediates when testing drug-treated cells because fork progression is limited in HU, as

elongation of DNA synthesis from ARSs is slow⁶⁵, thus, all replication intermediates detected under our experimental conditions by 2D gel analysis belong to the closest origin of replication for any given restriction fragment tested. Consistent with the idea that non-canonical/small Ys might be pathological replication structures, both *fen1^{rad27}* and *cdc9-7* mutants accumulate small Ys (comparable to *top1 top2* double mutants⁶⁶) compatible with increased accumulation of nicked DNA, therefore, fragile molecules.

The suppression of the accumulation of these non-canonical molecules in HU-treated cells by *POL30* disassembly-prone mutant alleles, *pol30^{R14E}* and *pol30^{D150E}*, combined with the suppression of the slow bulk DNA replication, show that *ubp10Δ* mutation have an effect throughout the entire yeast genome. All this evidence indicates that this Ubp10 deubiquitylase plays a significant genome-wide role during the S phase of every unperturbed cell cycle.

PCNA trimer-disassembly-prone mutants *pol30^{R14E}* and *pol30^{D150E}* alleviate the Okazaki fragment length extension problem described in *elg1Δ* cells⁵⁵. Further, combining *pol30^{R14E}* with *elg1Δ* largely rescued the elevated mutation rate of the single *elg1* mutant⁵⁸. Although *UBP10* mutant cells accumulate OFs, they do not show an elevated mutation rate, in fact their mutation rate is similar to that of wild-type cells^{36,43}. Both *pol30^{D150E}* and *pol30^{R14E}* PCNA mutant alleles are excellent extragenic suppressors of *UBP10* deletion. It has been described that due to their disassembly-prone nature of the homo-trimeric PCNA ring, both *POL30* alleles accumulate low levels of PCNA on replicating chromatin. However, based in our own observations, *pol30^{R14E}* and *pol30^{D150E}* point mutant alleles differ between them in the total cellular amount of PCNA levels. In whole cell extracts, PCNA^{D150E} levels mimics those of wild-type cells, while PCNA^{R14E} shows significantly reduced levels as compared to PCNA^{wt}. Thus, PCNA^{D150E} behaves like a real prone-disassembly PCNA mutant. Nevertheless, PCNA^{R14E} mirrors PCNA^{D150E} low levels of PCNA bound to chromatin and, therefore, it is meaningful in our analysis.

In summary, disassembly-prone mutants *pol30^{R14E}* and *pol30^{D150E}* rescue the chromatin retention of PCNA phenotype of *ubp10Δ* (as shown in Fig. 6a), as well as cell cycle delay (Figs. 5c, 6b) and defective replication intermediate accumulation upon exposure to HU (Fig. 5d). Remarkably, the *pol30^{D150E}* disassembly-prone mutant also rescues Okazaki fragments accumulation observed in DNA ligase I (*cdc9ts*) when combined with *ubp10Δ* (Fig. 6c). In other words, all major S phase phenotypes associated with defective Ubp10 (*ubp10Δ*) are relieved by reversion of accretion of PCNA by two different trimer instability PCNA/*POL30* mutants (*pol30^{R14E}* and *pol30^{D150E}*)^{55,58}. Together, this evidence indicates that a slow PCNA unloading underlies every replication defect in Ubp10 depleted cells.

The analysis of *fen1Δ ubp10Δ* mutants revealed the epistatic nature of their genetic interaction, where the loss of Fen1 suppresses the *ubp10* phenotype (as evidenced by all tests, including the characteristic accumulation of PCNA on chromatin observed in *fen1Δ* mutants). This suggests that the flap endonuclease activity of Fen1^{Rad27} is necessary to generate an Okazaki fragment maturation intermediate upon which Ubp10 acts. In Fen1 depleted cells, the Ubp10-dependent mechanism would not unload the sliding clamp, potentially directing PCNA entirely to the Elg1-dependent pathway, thereby preventing its hyperaccumulation on chromatin. Conversely, Fen1's activity on Okazaki fragments might commit PCNA for unloading by Ubp10, making it resistant to Elg1, which leads to the accumulation of PCNA on chromatin in FEN1 wild-type *ubp10Δ* cells.

Another relevant information here is that Elg1-depleted cells transiently accumulate PCNA on chromatin (Fig. 7). This transient nature of PCNA retention on chromatin is, on one hand, consistent with the viability of *elg1Δ* deleted strains²³⁻²⁵. However, on the other hand, it may also mean that in the absence of Elg1-RLC complex PCNA is steadily unloaded in vivo, as we show here (Fig. 7). Although it does not come as a total surprise, this unanticipated observation is coherent

with the fact that Elg1 is not essential for DNA replication^{23–25}. Nonetheless, as reported, Elg1 may be still important for efficient S phase progression or in the presence of replication stress¹⁸. However, by testing bulk DNA replication in unperturbed conditions at 25 °C, we observed no S phase delays in Elg1-depleted cells (in similar conditions where we detected a transient accretion of chromatin-bound PCNA). One possibility is that under these experimental circumstances an alternative complex to Elg1-RLC1 is unloading PCNA.

The transient accumulation of chromatin-bound PCNA in *elg1Δ* cells is, therefore, evocative of the existence of a PCNA unloading mechanism active during replication. We show here that only when *elg1Δ* is combined with *ubp10Δ* PCNA remains bound onto chromatin. Interestingly, we detected a robust accumulation and a very slow-paced PCNA unloading in *elg1 ubp10* double-mutant cells in synchronized S phase, suggesting the existence of an Ubp10-regulated PCNA chromatin dissociation mechanism divergent from that of Elg1-RLC. Undeniably, while alternative interpretations are possible, all the evidence suggests that a Ubp10-dependent mechanism supports timely removal of PCNA from replicating chromatin during unperturbed S phase. Eventually, PCNA is unloaded in Elg1 and Ubp10 doubly-depleted cells, as chromatin-bound PCNA in G1 synchronized cells remains very low. Perhaps most significantly, S phase progression is slow in this *elg1 ubp10* double mutant. The fact that depletion of Ubp10 has a similar slow S phase phenotype may be indicative of a default mechanism of PCNA unloading regulated by this PCNA-DUB in unperturbed cell cycle.

Although we cannot rule out alternative explanations, our results point at the existence of a PCNA chromatin dissociation route enabled and/or enhanced by Ubp10. If that were the case, it would be of interest to identify and functionally characterize additional factors involved in this novel, and likely Elg1-independent, mechanism.

Kubota et al., predicted Elg1-RLC alternative PCNA unloaders back in 2013²⁶. In fact, they suggested three models of PCNA unloading based on published evidence at the time and still valid today. A first model where Elg1-RLC would be the main unloader; a second model where Rfc1-RFC would work as a genome-wide unloader and Elg1-RLC would be the unloader of PCNA at specific genome localizations with emphasis in difficult to replicate sites; and a third model where Elg1-RLC complex would unload SUMOylated PCNA and Rfc1-RFC would unload unmodified PCNA rings to directly recycle them at lagging strands. Our findings are consistent with the last two models yet better support the third one where two different PCNA unloaders complexes would effectively recycle PCNA during the synthesis of lagging strands (model in Fig. 8). We suggest that the most likely alternative PCNA unloader is Rfc1-RFC, and that it may unload PCNA preferentially when deubiquitylated. Rfc1 is an essential subunit of the RFC complex that interacts with Ubp10 and PCNA. Ubp10 would eventually regulate the precise timing of PCNA unloading by Rfc1-RFC after Ub-PCNA^{K164} deubiquitylation. Our working model predicts that PCNA is ubiquitylated at K164 at lagging strands (Fig. 8), we hypothesize that such event would be a consequence of the collision of the PCNA-Pol δ complex with the preceding (5' end) Okazaki Fragment. Prior to Ubp10 action and subsequent PCNA unloading, PCNA ubiquitylation would enhance Pol δ release by a collision-release mechanism already described⁴⁷.

A strong case can be made here that yeast cells coordinate the last steps of synthesis and maturation of Okazaki fragments through a Ubp10-regulated PCNA unloading mechanism (see model in Fig. 8). Our findings are consistent with the hypothesis that *S. cerevisiae* cells ubiquitylate and deubiquitylate PCNA during S phase in a dynamic, yet ordered, manner to ensure normal DNA replication, such that PCNA ubiquitylation is orderly followed by its deubiquitylation to strengthen PCNA unloading at lagging strands in a genome-wide scale, regulating and ensuring the time frame for Okazaki fragments maturation to generate a continuous lagging double-stranded DNA.

Methods

Yeast strains, growth conditions and media

All the budding yeast used in this study originate from a *MATa* W303 *RADS bar1::LEU2* strain³⁶ and are listed in Supplementary table 1. Budding yeast strains were grown in YPAD medium (1% yeast extract, 2% peptone supplemented with 50 μ g/ml adenine) containing 2% glucose. For block-and-release experiments, cells were grown in YPAD with 2% glucose at 25 °C and synchronized in G1 with α -factor pheromone (40 ng/ml, 2.5 h). Cells were then collected by centrifugation (800 x g, 3 min) and released into fresh media (supplemented with 50 μ g/ml of Pronase) in the absence or in the presence of HU (0.2 M, FORMEDIUM). Overexpression experiments with cells grown in YPAD medium with 2% raffinose at 25 °C were conducted by adding to the medium 2.5% galactose (to induce) or 2% glucose (to repress).

General experimental procedures

General experimental procedures of yeast Molecular and Cellular Biology, and generation of tagged alleles and specific gene deletions were performed as described^{61,68–70}. Transformation was performed by lithium acetate protocol and transformants were selected by growing in selective mediums. Different selection markers were used (*KANMX6*, *HphMX4*, *NatMX6*, *URA3*, *TRP1*, *HIS3*), as indicated in Supplementary table 1. Constructs were confirmed by PCR and/or sequencing. The presence of tagged proteins was further confirmed by immunoblot. Moreover, strains with tagged alleles were carefully checked for growth rate and sensitivity to HU. No differences with untagged controls were found. Some mutant strains, such as the *cdc9-7* background, are genetically unstable and can give raise to revertants, contributing to experimental variability. To avoid this, once strains are thawed, single colonies were isolated and tested for *cdc9-7* in terms of its thermosensitivity phenotype, just before to perform the experiments. All reagent information (antibodies, chemical peptides, recombinant proteins and oligonucleotides) is detailed in the Supplementary Tables 1 and 2.

Flow Cytometry Analysis

For flow cytometry analysis, 10⁷ cells were collected by centrifugation, washed once with water, fixed in 70% ethanol and processed for DNA analysis⁷¹. DNA content was determined by using SYTOX Green (Molecular PROBES) for DNA staining^{72,73}. The DNA content of individual cells was measured using a Becton Dickinson Accuri C6 plus software. A minimum of 10.000 cells were scored per time-point.

HU and temperature sensitivity assays

Stationary cells were counted and serially diluted in YPAD media. Ten-fold dilutions of equal numbers of cells were plated onto YPAD (2% glucose) media (always supplemented with 50 μ g/ml adenine), or YPAD containing HU, incubated at the indicated temperatures for 24, 48, 72 or 120 h and then scanned using Epson Easy Photo FixTM (v.3.9.2.0ES) software.

Identification of Ubp10 interactors by mass spectrometry

Ubp10-GFP expressing- and untagged control cells were synchronized with α -factor and released into fresh YPAD. 30 min, 40 min, 50 min and 60 min time point samples were fixed with formaldehyde and harvested. Cell pellets were resuspended in Lysis Buffer (50 mM Hepes pH 7.5, 140 mM NaCl, 1 mM EDTA, 1% Triton-X100, 0.1% Na-deoxycholate) and broken using glass beads in a fast-prep. Chromatin extracts were disrupted by sonication, cleared by centrifugation, and incubated for 4 h at 4 °C with agarose-conjugated GFP-Trap™ beads (Chromotek). Beads were washed once with lysis buffer, once with Wash Buffer (10 mM Tris pH 8, 250 mM LiCl, 1 mM EDTA, 0.5% NP-40, 0.5% Na-deoxycholate) and once with TE. 30 min, 40 min, 50 min and 60 min samples corresponding to each strain (Ubp10-GFP expressing cells and untagged control cells) were pulled and the two resulting samples

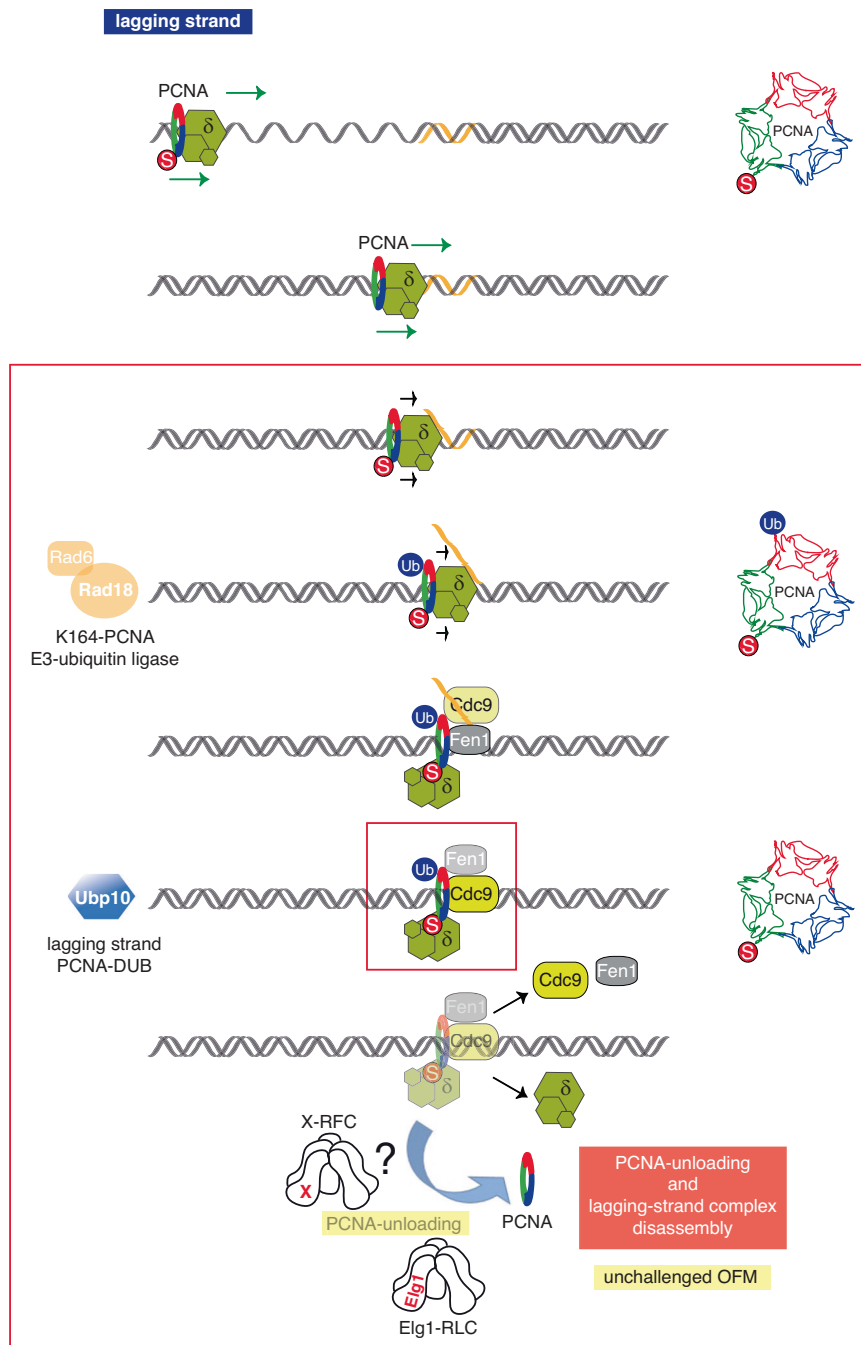


Fig. 8 | Model for Okazaki fragment maturation through dynamic ubiquitylation and deubiquitylation of PCNA Lysine 164. Ubp10-mediated deubiquitylation of K164-PCNA triggers a PCNA chromatin unloading mechanism at the final steps of the synthesis and ligation of DNA at lagging strands (see Discussion text for details).

resuspended in Laemmli Buffer, resolved by SDS-PAGE and silver stained. Regions of interest were excised, destained and digested with modified porcine trypsin (Promega, Madison, Wis.)⁷⁴. Tryptic peptides were recovered, dried in a speed vacuum system, and desalted by using C18-homemade microcolumns. A nano-UHPLC system (NanoE-lute, Bruker Daltonics, Germany) coupled to a hybrid trapped ion mobility-quadrupole time-of-flight mass spectrometer Tims TOF Pro (Bruker Daltonics, Germany) via a modified nano-electrospray ion source (Captive Spray, Bruker Daltonics, Germany) was used for reversed-phase LC-MS/MS analysis. Peptides were dissolved in 0.1%FA/2%ACN and loaded onto a trapping column (Trap AcclaimPepMap 100 C18, Thermo) and were separated on a C18 1.9 μ m 75ID 15 cm column (nanoElute FIFTEEN, Bruker Daltonics) at 40 °C using a 60 min

gradient (from 2% to 35% ACN/0.1 FA) at a flow rate of 300 nL/min. MS acquisition was run in data-dependent acquisition (DDA) mode with PASEF. The acquired data were submitted to the MaxQuant (1.6.17.0) quantitative proteomics software package for identification and relative quantification by iBAQ and MaxLFQ.

The UniProtKB database has been used using the reviewed sequences and isoforms from the *Saccharomyces cerevisiae* proteome (UP 000002311 download 2022-02-22).

Search parameters were as follows: fully tryptic digestion with up to two missed cleavages, 40 ppm and 20 ppm mass tolerances for precursor and product ions, respectively, oxidation of methionine and acetylation of the protein N-terminus were established as variable modifications and carbamidomethylation of cysteine as fixed

modification, and seven amino acids minimum peptide length. One percent false discovery rate (1% FDR) using Target-Decoy database for both peptide and protein validation. For protein identification one unique peptide was considered as the minimum number. This experiment was performed once ($n=1$). This proteomic analysis was performed in the Proteomics Facility of the Cancer Research Center (Salamanca, Spain). The mass spectrometry proteomics data have been deposited to the ProteomeXchange Consortium via the PRIDE⁷⁵ partner repository with the dataset identifier [PXD048249](https://doi.org/10.1038/s41467-024-52542-9).

Total protein extracts for Immunoblotting

Total protein extracts were prepared following cell fixation using trichloroacetic acid (TCA) and resolved by SDS-polyacrylamide gel electrophoresis before transfer to nitrocellulose membranes.

Fractioning and Immunoblotting

For chromatin-enriched fractions around 6×10^7 exponentially growing cells were harvested by centrifugation and resuspended in 1 ml of Buffer 1 (containing 150 mM Tris pH 8.8, 10 mM dithiothreitol (DTT), and 0.1% sodium azide), and incubated at room temperature for 10 min. Cells were pelleted, washed with 1 ml of Buffer 2 (50 mM $\text{KH}_2\text{PO}_4/\text{K}_2\text{HPO}_4$ pH 7.4, 0.6 M Sorbitol, and 10 mM DTT), resuspended in 200 μl of Buffer 2 supplemented with 40 μg Zymolyase-100T and incubated at 37 °C for 10 min with intermittent mixing. The resulting spheroplasts were washed with 1 ml of ice-cold Buffer 3 (50 mM HEPES pH 7.5, 100 mM KCl, 2.5 mM MgCl, and 0.4 M Sorbitol), followed by resuspension and a 5-min incubation in 100 μl of EBX buffer (50 mM HEPES pH 7.5, 100 mM KCl, 2.5 mM MgCl, 0.25% Triton100, 1 mM phenylmethylsulfonyl fluoride (PMSF), Protease inhibitor tablets (EDTA-free, Roche), Leupeptin 1 $\mu\text{g}/\text{ml}$, Pepstatin 2.5 $\mu\text{g}/\text{ml}$, and RNase 10 $\mu\text{g}/\text{ml}$), with occasional mixing. Aliquots of 30 μl of these disrupted cell suspensions were collected as whole cell extract samples (WCE). Remaining volume was layered onto 70 μl of cold EBX-S buffer (EBX buffer supplemented with 30% Sucrose) and subjected to centrifugation at 13,500 \times g for 10 min at 4 °C. Aliquots of 30 μl of the resulting supernatant layer (Chromatin-free fraction) were also collected. After discarding supernatant, chromatin pellets were washed with 200 μl of EBX-S buffer, resuspended in 70 μl of EBX buffer supplemented with 0.5 μl of Benzonase, and incubated on ice for 15 min (Chromatin fraction). SDS-PAGE loading buffer was added to each fraction.

The different protein extracts were separated by SDS-polyacrylamide gel electrophoresis and transferred to nitrocellulose membranes. Antibodies used for detection are listed in the Supplementary table 2 and were visualized using ECL reagents (Amersham Pharmacia Biotech) and films (FujiFilm). The levels of proteins bound to chromatin were quantified using Quantity One (v.4.6.6) Software (BioRad) and normalized with their corresponding Histone H2B values. All data in the bar graphs are presented as means SD in triplicate. Statistical analyzes were conducted with GraphPad Prism (v.10.1.0). A two-way analysis of variance (ANOVA) test was used to determine the statistical significance.

Protein interaction analysis

Cells expressing tagged or untagged (control) proteins were fixed with 1% formaldehyde and harvested. Chromatin extracts were prepared in a Lysis Buffer containing 50 mM Hepes pH 7.5, 140 mM NaCl, 1 mM EDTA, 1% Tritón-X100, 0.1% Na-deoxycholate, and supplemented with Antiproteolytic Cocktail using glass beads. Extracts were cleared by centrifugation; soluble protein fractions were discarded, and chromatin pellets were sheared by sonication. Chromatin extracts were clarified and tagged proteins were enriched by immunoprecipitation with specific Tag antibodies previously bound to Protein G Dynabeads (5 h at 4 °C). Then, antibody-bound Protein G Dynabeads and controls were extensively washed with lysis buffer, and elution was carried out in SDS-PAGE loading buffer. Immunoprecipitates were resolved by

SDS-PAGE gels, transferred to nitrocellulose membranes and analyzed with specific-HRP conjugated antibodies.

Okazaki fragment analysis

Cells were collected by centrifugation, washed in SCE buffer (1 M sorbitol, 100 mM sodium citrate, 60 mM EDTA, pH 7.0) and spheroblsted for 3 min with 5 mg zymolyase 20 T (Amsbio) per 50 ml culture. Spheroblast were washed with SCE, resuspended by gently pipetting in 490 μl lysis buffer (50 mM Tris-HCl, pH 8.0, 50 mM EDTA, 100 mM NaCl, 1.5% sarkosyl) containing 150 μg proteinase K (Sigma-Aldrich) and digested for 14 h at 37 °C. Residual proteins and peptides were precipitated by adding 200 μl 5 M KOAc and centrifugation at 16,000 \times g for 30 min at 4 °C. Nucleic acids were obtained from the supernatant by precipitation with isopropanol and centrifugation at 16,000 \times g for 10 min at 4 °C. Pellets were washed with 70% ethanol, air dried, resuspended in 200 μl STE buffer (10 mM Tris-HCl, pH 8.0, 1 mM EDTA, 100 mM NaCl) and digested with 25 μg RNase A (Sigma-Aldrich) at 37 °C for 1 h. DNA was precipitated by addition of 20 μl NaOAc (pH 5.2) and 800 μl ethanol followed by centrifugation at 5000 \times g for 10 min at 25 °C. DNA pellets were washed with 70% ethanol, air dried and resuspended in 1 μl TE/ml original culture volume. For DNA labeling, 2 μl of the DNA obtained was used in 20 μl labeling reactions containing 1U Klenow (exo-)polymerase (NEB) and 0.4 μl of $\alpha\text{-}^{32}\text{P}$ -dCTP (Perkin Elmer). Reactions were incubated at 37 °C for 30 min. Free label was removed using Illustra microspin G-50 columns (GE healthcare). Labeled DNA was resolved in 1.3% denaturing agarose gels (50 mM NaOH, 1 mM EDTA). After electrophoresis, the gel was neutralized, and DNA transferred to an uncharged nitrocellulose membrane (Hybond-N; GE healthcare) by capillary transfer. Membranes were exposed to phospho screens (Fujifilm BAS-MS). Images were acquired using a Molecular Imager FX (BioRad).

Two-dimensional DNA gels

Cell cultures were mixed with ice-cold AZ-STOP solution (0.5 M NaOH, 0.4 M EDTA, 0.2% Sodium Azide) in a 2:1 ratio, shaken vigorously, and collected by centrifugation at 2,300 \times g. Cell pellets were washed once with ice-cold water and then frozen before further processing. The cells were resuspended in 5 ml of NIB buffer (17% Glycerol, 50 mM MOPS, 150 mM potassium acetate, 2 mM MgCl_2 , 500 mM Spermidine, 150 μM Spermine) and disrupted by vortexing with an equal volume of pre-cooled glass beads (30 seconds at maximum power – 30 seconds on ice, 16–18 cycles). Breakage was confirmed by microscopy. The supernatant was recovered with a Pasteur pipette and centrifuged at 6000 \times g for 10 min at 4 °C. Pellets were resuspended in 5 ml of G2 Buffer (Quiagen) using a 1 ml cut pipette tip. 100 μl of RNase (10 mg/ml) were added, and the samples were incubated for 45 min at 37 °C. Next, 100 μl of Proteinase K (20 mg/ml) were added, and samples were incubated for 1 h at 37 °C. Samples were clarified by centrifugation (2300 \times g, 5 min at 4 °C) and 5 ml of QBT buffer (Quiagen) was added. DNA samples were then purified using Genomic-Tip 100/G columns (Quiagen) and precipitated with Isopropyl alcohol. Samples were centrifuged (21,000 \times g, 30 min at 4 °C), and DNA pellets were washed with cold EtOH 80%, left to air dry, and resuspended in TE. DNA was digested with the NcoI restriction enzyme and subjected to first-dimension electrophoresis (0.4% agarose in TBE buffer, 20 V for 36 h at room temperature). Gel slices containing samples were excised, rotated 90° counterclockwise with respect to the first dimension, and placed in a gel-casting tray for second-dimension electrophoresis (1% agarose in TBE buffer containing 500 ng/ml Ethidium bromide, 160 V for 4.5 h at 4 °C). After denaturing with 0.4 M NaOH for 20 min, samples were transferred to nitrocellulose membrane Hybond-XL (GE Healthcare) by capillary transfer and hybridized to radiolabeled probes spanning the *ARS305* and *ARS306* origins of DNA replication. For each origin of replication tested, the specific probe corresponds to the following coordinates (retrieved from SGD): *ARS305* (39073-40557, Chr III) and *ARS306* (73001-73958, Chr III). PCR

oligonucleotides used to generate them are listed in the Resources Table (Supplementary Information). Images were acquired using a Molecular Imager FX (BioRad) and the different replication-associated DNA molecules were quantified using Quantity One (v.4.6.6) software (BioRad).

Reporting summary

Further information on research design is available in the Nature Portfolio Reporting Summary linked to this article.

Data availability

Yeast strains generated in this study are available on request from the corresponding authors. The raw mass spectrometry proteomics data have been deposited to the ProteomeXchange Consortium via the PRIDE⁷⁵ partner repository with the dataset identifier [PXD048249](https://doi.org/10.1093/bioinformatics/btad048). Source data are provided with this paper.

References

- Moldovan, G.-L., Pfander, B. & Jentsch, S. PCNA, the maestro of the replication fork. *Cell* **129**, 665–679 (2007).
- Bell, S. P. & Labib, K. Chromosome duplication in *Saccharomyces cerevisiae*. *Genetics* **203**, 1027–1067 (2016).
- Zheng, L. & Shen, B. Okazaki fragment maturation: nucleases take centre stage. *J. Mol. Cell Biol.* **3**, 23–30 (2011).
- Acharya, N., Klassen, R., Johnson, R. E., Prakash, L. & Prakash, S. PCNA binding domains in all three subunits of yeast DNA polymerase δ modulate its function in DNA replication. *Proceedings of the National Academy of Sciences* <https://doi.org/10.1073/pnas.1109981108> (2011).
- Vijayakumar, S. et al. The C-terminal domain of yeast PCNA is required for physical and functional interactions with Cdc9 DNA ligase. *Nucleic acids Res.* **35**, 1624–1637 (2007).
- Gary, R. et al. A Novel Role in DNA Metabolism for the Binding of Fen1/Rad27 to PCNA and Implications for Genetic Risk. *Mol. Cell Biol.* **19**, 5373–5382 (1999).
- Shibahara, K. & Stillman, B. Replication-dependent marking of DNA by PCNA facilitates CAF-1-coupled inheritance of chromatin. *Cell* **96**, 575–585 (1999).
- Ulrich, H. D. New insights into replication clamp unloading. *J. Mol. Biol.* **425**, 4727–4732 (2013).
- Arbel, M., Liefshitz, B. & Kupiec, M. How yeast cells deal with stalled replication forks. *Curr. Genet* **66**, 911–915 (2020).
- Cullmann, G., Fien, K., Kobayashi, R. & Stillman, B. Characterization of the five replication factor C genes of *Saccharomyces cerevisiae*. *Mol. Cell Biol.* **15**, 4661–4671 (1995).
- Yao, N. et al. Replication factor C clamp loader subunit arrangement within the circular pentamer and its attachment points to proliferating cell nuclear antigen. *J. Biol. Chem.* **278**, 50744–50753 (2003).
- Bermudez, V. P. et al. The alternative Ctf18-Dcc1-Ctf8-replication factor C complex required for sister chromatid cohesion loads proliferating cell nuclear antigen onto DNA. *Proc. Natl Acad. Sci.* **100**, 10237–10242 (2003).
- Lengronne, A. et al. Establishment of sister chromatid cohesion at the *S. cerevisiae* replication fork. *Mol. Cell* **23**, 787–799 (2006).
- Liu, H. W. et al. Division of labor between PCNA Loaders in DNA replication and sister chromatid cohesion establishment. *Mol. Cell* **78**, 725–738.e4 (2020).
- Cai, J. et al. Reconstitution of human replication factor C from its five subunits in baculovirus-infected insect cells. *Proc. Natl Acad. Sci.* **93**, 12896–12901 (1996).
- Yao, N. et al. Clamp loading, unloading and intrinsic stability of the PCNA, β and gp45 sliding clamps of human, *E. coli* and T4 replicases. *Genes Cells* **1**, 101–113 (1996).
- Bylund, G. O. & Burgers, P. M. J. Replication protein A-directed unloading of PCNA by the Ctf18 cohesion establishment complex. *Mol. Cell Biol.* **25**, 5445–5455 (2005).
- Kubota, T., Nishimura, K., Kanemaki, M. T. & Donaldson, A. D. The Elg1 replication factor C-like complex functions in PCNA unloading during DNA replication. *Mol. Cell* **50**, 273–280 (2013).
- Lee, K., Fu, H., Aladjem, M. I. & Myung, K. ATAD5 regulates the lifespan of DNA replication factories by modulating PCNA level on the chromatin. *The Journal of Cell Biology* <https://doi.org/10.1083/jcb.201206084> (2012).
- Shiomi, Y. & Nishitani, H. Alternative replication factor C protein, Elg1, maintains chromosome stability by regulating PCNA levels on chromatin. *Genes Cells* **18**, 946–959 (2013).
- Kubota, T., Katou, Y., Nakato, R., Shirahige, K. & Donaldson, A. D. Replication-Coupled PCNA Unloading by the Elg1 Complex Occurs Genome-wide and Requires Okazaki Fragment Ligation. *Cell Reports* 1–15 <https://doi.org/10.1016/j.celrep.2015.06.066> (2015).
- Shiomi, Y. & Nishitani, H. Control of genome integrity by RFC complexes: conductors of PCNA loading onto and unloading from chromatin during DNA replication. *Genes* **8**, 52 (2017).
- Ben-Aroya, S., Koren, A., Liefshitz, B., Steinlauf, R. & Kupiec, M. ELG1, a yeast gene required for genome stability, forms a complex related to replication factor C. *Proc. Natl Acad. Sci. USA* **100**, 9906–9911 (2003).
- Bellaoui, M. et al. Elg1 forms an alternative RFC complex important for DNA replication and genome integrity. *EMBO J.* **22**, 4304–4313 (2003).
- Kanellis, P., Agyei, R. & Durocher, D. Elg1 forms an alternative PCNA-interacting RFC complex required to maintain genome stability. *Curr. Biol.* **13**, 1583–1595 (2003).
- Kubota, T., Myung, K. & Donaldson, A. D. Is PCNA unloading the central function of the Elg1/ATAD5 replication factor C-like complex? *Cell cycle (Georget., Tex.)* **12**, 2570–2579 (2013).
- Hoegge, C., Pfander, B., Moldovan, G.-L., Pyrowolakis, G. & Jentsch, S. RAD6-dependent DNA repair is linked to modification of PCNA by ubiquitin and SUMO. *Nature* **419**, 135–141 (2002).
- Mailand, N., Gibbs-Seymour, I. & Bekker-Jensen, S. Regulation of PCNA-protein interactions for genome stability. *Nat. Rev. Mol. Cell Biol.* **14**, 269–282 (2013).
- Chang, D. J. & Cimprich, K. A. DNA damage tolerance: when it's OK to make mistakes. *Nat. Chem. Biol.* **5**, 82–90 (2009).
- Friedberg, E. C. Suffering in silence: the tolerance of DNA damage. *Nat. Rev. Mol. Cell Biol.* **6**, 943–953 (2005).
- Hedglin, M. & Benkovic, S. J. Regulation of Rad6/Rad18 activity during DNA damage tolerance. *Annu. Rev. biophysics* **44**, 207–228 (2015).
- Stelter, P. & Ulrich, H. D. Control of spontaneous and damage-induced mutagenesis by SUMO and ubiquitin conjugation. *Nature* **425**, 188–191 (2003).
- Huang, T. T. et al. Regulation of monoubiquitinated PCNA by DUB autocleavage. *Nat. Cell Biol.* **8**, 341–347 (2006).
- Kashiwaba, S. et al. USP7 is a suppressor of PCNA ubiquitination and oxidative-stress-induced mutagenesis in human cells. *Cell Reports* 1–10 <https://doi.org/10.1016/j.celrep.2015.11.014> (2015).
- Lim, K. S. et al. USP1 is required for replication fork protection in BRCA1-deficient tumors. *Mol. Cell* **72**, 925–941.e4 (2018).
- Gallejo-Sánchez, A., Andrés, S., Conde, F., San-Segundo, P. A. & Bueno, A. Reversal of PCNA ubiquitylation by Ubp10 in *Saccharomyces cerevisiae*. *PLoS Genet.* **8**, e1002826 (2012).
- Álvarez, V. et al. PCNA deubiquitylases control DNA damage bypass at replication forks. *Cell Reports* **29**, 1323–1335.e5 (2019).
- Emre, N. C. T. et al. Maintenance of low histone ubiquitylation by Ubp10 correlates with telomere-proximal Sir2 association and gene silencing. *Mol. Cell* **17**, 585–594 (2005).
- Gardner, R. G., Nelson, Z. W. & Gottschling, D. E. Ubp10/Dot4p regulates the persistence of ubiquitinated histone H2B: distinct

- roles in telomeric silencing and general chromatin. *Mol. Cell. Biol.* **25**, 6123–6139 (2005).
40. Schulze, J. M. et al. Splitting the task: Ubp8 and Ubp10 deubiquitinate different cellular pools of H2BK123. *Genes Dev.* **25**, 2242–2247 (2011).
41. Richardson, L. A. et al. A conserved deubiquitinating enzyme controls cell growth by regulating RNA polymerase I stability. *Cell Reports* <https://doi.org/10.1016/j.celrep.2012.07.009> (2012).
42. Mapa, C. E., Arsenault, H. E., Conti, M. M., Poti, K. E. & Benanti, J. A. A balance of deubiquitinating enzymes controls cell cycle entry. *Mol. Biol. Cell* **29**, 2821–2834 (2018).
43. Álvarez, V. et al. Orderly progression through S-phase requires dynamic ubiquitylation and deubiquitylation of PCNA. *Sci. Rep.* **6**, 25513 (2016).
44. Daigaku, Y. et al. PCNA ubiquitylation ensures timely completion of unperturbed DNA replication in fission yeast. *PLoS Genet.* **13**, e1006789 (2017).
45. Thakar, T. et al. Ubiquitinated-PCNA protects replication forks from DNA2-mediated degradation by regulating Okazaki fragment maturation and chromatin assembly. *Nat. Commun.* **11**, 2147–14 (2020).
46. Becker, J. R. et al. Genetic interactions implicating postreplicative repair in Okazaki fragment processing. *PLoS Genet.* **11**, e1005659 (2015).
47. Guillian, T. A. & Yeeles, J. T. P. Reconstitution of translesion synthesis reveals a mechanism of eukaryotic DNA replication restart. *Nat. Struct. Mol. Biol.* **27**, 450–460 (2020).
48. Nune, M. et al. FACT and Ubp10 collaborate to modulate H2B deubiquitination and nucleosome dynamics. *eLIFE* 1–24 <https://doi.org/10.7554/elife.40988.001> (2019).
49. Johnston, L. H. & Nasmyth, K. A. *Saccharomyces cerevisiae* cell cycle mutant *cdc9* is defective in DNA ligase. *Nature* **274**, 891–893 (1978).
50. Smith, D. J. & Whitehouse, I. Intrinsic coupling of lagging-strand synthesis to chromatin assembly. *Nature* **483**, 434–438 (2012).
51. Blair, K. et al. Mechanism of human Lig1 regulation by PCNA in Okazaki fragment sealing. *Nat. Commun.* **13**, 7833 (2022).
52. Kachroo, A. H. et al. Evolution. systematic humanization of yeast genes reveals conserved functions and genetic modularity. *Sci. (N. Y., NY)* **348**, 921–925 (2015).
53. Unternährer, S. & Hinnen, A. Temperature sensitivity of the *cdc9-1* allele of *Saccharomyces cerevisiae* DNA ligase is dependent on specific combinations of amino acids in the primary structure of the expressed protein. *Mol. Gen. Genet. MGG* **232**, 332–334 (1992).
54. Kahli, M., Osmundson, J. S., Yeung, R. & Smith, D. J. Processing of eukaryotic Okazaki fragments by redundant nucleases can be uncoupled from ongoing DNA replication in vivo. *Nucleic Acids Res.* **47**, 1814–1822 (2019).
55. Gali, V. K. et al. Identification of Elg1 interaction partners and effects on post-replication chromatin re-formation. *Plos Genet* **14**, e1007783 (2018).
56. Sriskanda, V., Schwer, B., Ho, C. K. & Shuman, S. Mutational analysis of *Escherichia coli* DNA ligase identifies amino acids required for nick-ligation in vitro and for in vivo complementation of the growth of yeast cells deleted for CDC9 and LIG4. *Nucleic Acids Res* **27**, 3953–3963 (1999).
57. Canas, J. C. et al. Strand asymmetry of DNA damage tolerance mechanisms. *BioRxiv* <https://doi.org/10.1101/2024.01.21.576515> (2024).
58. Devakumar, L. J. P. S., Gaubitz, C., Lundblad, V., Kelch, B. A. & Kubota, T. Effective mismatch repair depends on timely control of PCNA retention on DNA by the Elg1 complex. *Nucleic Acids Res* **47**, 6826–6841 (2019).
59. Kang, M.-S. et al. Regulation of PCNA cycling on replicating DNA by RFC and RFC-like complexes. *Nat. Commun.* **10**, 2420 (2019).
60. Katou, Y. et al. S-phase checkpoint proteins Tof1 and Mrc1 form a stable replication-pausing complex. *Nature* **424**, 1078–1083 (2003).
61. Calzada, A., Hodgson, B., Kanemaki, M., Bueno, A. & Labib, K. Molecular anatomy and regulation of a stable replisome at a paused eukaryotic DNA replication fork. *Genes Dev.* **19**, 1905–1919 (2005).
62. Nedelcheva, M. N. et al. Uncoupling of unwinding from DNA synthesis implies regulation of MCM helicase by Tof1/Mrc1/Csm3 checkpoint complex. *J. Mol. Biol.* **347**, 509–521 (2005).
63. Bando, M. et al. Csm3, tof1, and mrc1 form a heterotrimeric mediator complex that associates with DNA replication forks. *J. Biol. Chem.* **284**, 34355–34365 (2009).
64. Safaric, B. et al. The fork protection complex recruits FACT to reorganize nucleosomes during replication. *Nucleic Acids Res* **50**, gkac005 (2022).
65. Poli, J. et al. dNTP pools determine fork progression and origin usage under replication stress. *EMBO J.* **31**, 883–894 (2011).
66. Bermejo, R. et al. Top1- and Top2-mediated topological transitions at replication forks ensure fork progression and stability and prevent DNA damage checkpoint activation. *Genes Dev.* **21**, 1921–1936 (2007).
67. Langston, L. D. & O'donnell, M. DNA polymerase delta is highly processive with proliferating cell nuclear antigen and undergoes collision release upon completing DNA. *J. Biol. Chem.* **283**, 29522–29531 (2008).
68. Cordon-Preciado, V., Ufano, S. & Bueno, A. Limiting amounts of budding yeast Rad53 S-phase checkpoint activity results in increased resistance to DNA alkylation damage. *Nucleic Acids Res.* **34**, 5852–5862 (2006).
69. Sánchez, M., Calzada, A. & Bueno, A. The Cdc6 protein is ubiquitinated in vivo for proteolysis in *Saccharomyces cerevisiae*. *J. Biol. Chem.* **274**, 9092–9097 (1999).
70. Longtine, M. S. et al. Additional modules for versatile and economical PCR-based gene deletion and modification in *Saccharomyces cerevisiae*. *Yeast (Chichester, Engl.)* **14**, 953–961 (1998).
71. Calzada, A., Sacristán, M., Sánchez, E. & Bueno, A. Cdc6 cooperates with Sic1 and Hct1 to inactivate mitotic cyclin-dependent kinases. *Nature* **412**, 355–358 (2001).
72. Haase, S. B. & Reed, S. I. Improved flow cytometric analysis of the budding yeast cell cycle. *Cell cycle (Georget., Tex.)* **1**, 132–136 (2002).
73. Haase, S. B. Cell cycle analysis of budding yeast using SYTOX Green. *Current protocols in cytometry Chapter 7*, Unit 7.23-7.23.4 (2004).
74. Shevchenko, A., Wilm, M., Vorm, O. & Mann, M. Mass Spectrometric Sequencing of Proteins from Silver-Stained Polyacrylamide Gels. *Anal. Chem.* **68**, 850–858 (1996).
75. Perez-Riverol, Y. et al. The PRIDE database resources in 2022: a hub for mass spectrometry-based proteomics evidences. *Nucleic Acids Res* **50**, D543–D552 (2021).

Acknowledgements

We are grateful to members of O8 research group at the IBMCC for helpful discussions. We would like to particularly thank Professor Anne Donaldson and Takashi Kubota PhD (University of Aberdeen) for *pol30* mutant and ChVlig1 strains. We are also grateful to the National BioResource Project, NBRP Japan for the *cdc9-7* strain. This work was supported by the Spanish Ministry of Science (grants PID2019-109616GB-I00 to A.B. and M.P.S. and PID2020-116003GB-I00 to R.B.) and Junta de Castilla y León (grant SA103P20 to A.B.). J.Z. was supported by a Pre-doctoral Fellowship from the Junta de Castilla y León (JCyL). S.M. was supported by a University of Salamanca Postdoctoral Fellowship and a MSCA Postdoctoral Fellowship (grant n° 101106007). E.A. was supported by a JCyL Postdoctoral Fellowship. A.B. and M.P.S. Institution is supported by the “Programa de Apoyo a Planes Estratégicos de Investigación de Excelencia” cofunded by the Junta de Castilla y León and the European Regional Development Fund (CLC-2017-01).

Author contributions

Conceptualization, A.B., with substantial inputs from M.P.S., J.Z., S.M. and R.B.; Investigation, J.Z., S.M., E.A., M.A. S.R. and M.P.S.; Supervision, A.B. and M.P.S.; Formal Analysis, A.B., M.P.S., S.M. and J.Z.; Writing & Editing, A.B. and M.P.S. with the help of R.B. and S.M.; Funding Acquisition, A.B., M.P.S. and R.B.

Competing interests

The authors declare no competing interests.

Additional information

Supplementary information The online version contains supplementary material available at <https://doi.org/10.1038/s41467-024-52542-9>.

Correspondence and requests for materials should be addressed to María P. Sacristán or Avelino Bueno.

Peer review information *Nature Communications* thanks George-Lucian Moldovan and the other, anonymous, reviewer(s) for their contribution to the peer review of this work. A peer review file is available.

Reprints and permissions information is available at <http://www.nature.com/reprints>

Publisher's note Springer Nature remains neutral with regard to jurisdictional claims in published maps and institutional affiliations.

Open Access This article is licensed under a Creative Commons Attribution-NonCommercial-NoDerivatives 4.0 International License, which permits any non-commercial use, sharing, distribution and reproduction in any medium or format, as long as you give appropriate credit to the original author(s) and the source, provide a link to the Creative Commons licence, and indicate if you modified the licensed material. You do not have permission under this licence to share adapted material derived from this article or parts of it. The images or other third party material in this article are included in the article's Creative Commons licence, unless indicated otherwise in a credit line to the material. If material is not included in the article's Creative Commons licence and your intended use is not permitted by statutory regulation or exceeds the permitted use, you will need to obtain permission directly from the copyright holder. To view a copy of this licence, visit <http://creativecommons.org/licenses/by-nc-nd/4.0/>.

© The Author(s) 2024